TRIBHUVAN UNIVERSITY

INSTITUTE OF ENGINEERING

PULCHOWK CAMPUS

Thesis No: PUL075MSGtE006

Numerical Analysis of Pile wall for Excavation Support in Soft Ground

By

Madan Puri

A THESIS

SUBMITTED TO THE DEPARTMENT OF CIVIL ENGINEERING

IN PARTIAL FULFILLMENT OF THE REQUIREMENTS FOR THE

DEGREE OF MASTERS OF SCIENCE IN

GEOTECHNICAL ENGINEERING

DEPARTMENT OF CIVIL ENGINEERING

LALITPUR, NEPAL

June, 2023

COPYRIGHT

APPROVAL LETTER

TRIBHUVAN UNIVERSITY

INSTITUTE OF ENGINEERING

PULCHOWK CAMPUS

DEPARTMENT OF CIVIL ENGINEERING

The undersigned certify that they have read, and recommended to the Institute of Engineering for acceptance, a thesis entitled "**Numerical Analysis of Pile wall for Excavation Support in Soft Ground"** submitted by Mr. Madan Puri (PUL075MSGtE006) in partial fulfillment of the requirements for the degree of Master of Science in Geotechnical Engineering.

…….
Supervisor
Dr. Bhim Kumar Dahal
Assistant Professor
Institute of Engineering, Pulchowk Campus

…….
External Examiner
Dr. Mohan Prasad Acharya
Senior Geotechnical Engineer
NEA Engineering Company Ltd.

…….
Program Coordinator
Dr. Santosh Kumar Yadav
Institute of Engineering, Pulchowk Campus

ABSTRACT

Cantilever pile walls are a type of earth support structure that can provide advantages in minimizing excessive deformation during ground excavation. In multiple scenarios, the construction of basements for new buildings or structures is planned in close proximity to existing older buildings. In such instances, the surrounding area of the old building, known as the influence zone, exerts lateral earth pressure onto the newly excavated area. To withstand and contain this lateral earth pressure, a cantilever pile wall is constructed. Kathmandu, the capital and most populous city of Nepal, is characterized by buildings constructed on soft ground consisting of grey to dark silty clay and clayey silt. As the city moves towards the development of high-rise buildings, it becomes crucial to ensure proper excavation without causing any damage to the existing buildings in close proximity to the construction site. Therefore, well-designed cantilever piles are being studied using finite element analysis, considering both 2D and 3D modeling techniques. The objective is to analyze and design effective cantilever pile systems that can accommodate the requirements of the upcoming high-rise developments while safeguarding the nearby structures. The resulting straining effects, such as bending moments, shear forces, normal forces, and lateral support forces, can vary between 2D and 3D analyses. Additionally, the deformation of the wall and the subsidence profile may differ when comparing 2D and 3D analyses. Three different adjacent building foundation (isolated, strip and mat) were analyzed. The selection of a pile wall is commonly preferred and relatively straightforward for use in cohesive soil. A parametric study was conducted, taking into account soil properties, excavation depth, pile diameter, and embedded pile depth.

Keywords: Excavation, Cantilever pile wall, FEM, Adjacent building, PLAXIS 3D, 2D

ACKNOWLEDGEMENTS

I would like to especially express my sincere gratitude to my supervisors **Dr. Bhim Kumar Dahal**, for his motivation and proper guidance. This report would have never been accomplished without his assistance and dedicated involvement in every step throughout the process. His help over the course of this study was invaluable.

I am also grateful to **Dr. Santosh Kumar Yadav**, Pulchowk Campus, Institute of Engineering, Tribhuvan University, Nepal, for exposing me to academic research activities and for his encouragement.

I would like to thank all staffs of M. Sc. in Geotechnical Engineering program. I am equally thankful to my friends MSGtE/075 batch for their cooperation and intellect suggestions. My sincere thanks also go to all those who helped and gave valuable suggestions to me during the course of this research work.

My acknowledgement would be incomplete without thanking Er. Ritesh Baral, Dr. Mandip Subedi, Er. Rajan Kc and Er. Ayush Poudel. Their support and encouragement has resulted to in this achievement.

At last, but not the least, I would like to thank my family members and friends for their endless moral support and encouragement during my thesis study period. I owe all that I have accomplished up to this point of my life to them.

Madan Puri

PUL075/MSGtE/006

June, 2023

TABLE OF CONTENTS

List of Figures:

List of Tables:

1 INTRODUCTION

1.1 Background

When carrying out excavations in urban areas, it is crucial to carefully consider the effects of ground movements on nearby structures and utility systems. While both horizontal and vertical soil movements occur during excavation, the former is particularly crucial for adjacent support walls. These earth movements can lead to deformation and potential damage to nearby structures. To mitigate such risks, strict control over deformations is essential in urban excavation projects. When soft clays are present, the construction of robust excavation support walls becomes necessary to meet deformation control requirements. The necessary stiffness of the supporting wall is established based on the anticipated deformations and their potential impact on adjacent structures. Figure 1-1 depicts the problem at hand, showcasing lateral soil displacement towards the excavation, the bending of the supporting wall, and ground movement beneath a neighboring building as a result of excavation in clay soil. Differential settlement caused by soil displacement has the potential to cause substantial harm to surrounding structures. The severity of damage caused by excavation is influenced by several factors, including the type of structure, performance of the support wall, ground conditions, and construction activities. It is essential to employ different types of retaining structures, such as sheet pile walls, contiguous piles, secant piles, and diaphragm walls, in order to effectively prevent or reduce damage to neighboring buildings and underground utilities. Additionally, the excavation support wall experiences lateral soil movement, resulting in lateral forces. Hence, it holds significant importance to quantify or anticipate the magnitude of lateral displacement and its consequences on the supporting wall. The lateral stresses induced by soil movements create bending moments and deflections in the excavation supported by piles, potentially resulting in structural damage or failure in both the existing building and the support wall. (Ramadan et al., 2018).

According to (Poulos & Chen, 1997), there have been many reports discussing structural damage to piles.. Various theoretical and empirical techniques have been developed to address specific challenges encountered during excavations, as mentioned

by (Stewart et al., 1994)(Poulos et al., 1996)(Poulos & Chen, 1997). Cantilever walls are a suitable option for both temporary and permanent excavation work because they eliminate the need for internal struts, allowing for smoother construction progress. In soil mechanics textbooks, (Long et al., 2012) recommend excavations of up to 4.5 meters when employing cantilever walls. (Long, 2001) examined a database of cantilever wall cases from existing literature, while (Long et al., 2012) reported successful construction of 7.5-meter high cantilever walls in Dublin boulder clay, noting that these walls exhibited slower movement than anticipated. They suggested that cantilever walls should be used for higher retained heights, at least temporarily. The design of a pile wall supporting an excavation is influenced by various factors such as the depth of excavation, soil properties, and the foundation type and level of the adjacent building. ("Pile Foundation Analysis and Design," 1981) states that the secant modulus of elasticity ranges from 15 cu to 95 cu (where cu represents the undrained shear strength of clay), with lower values for very soft clay and higher values for stiff clay. For the current analysis, a value of 50 cu was used. Normally consolidated soft soils exhibit greater stiffness in the vertical direction than in the horizontal direction, according to (RHG, 1995). Ou's recommendation indicates that the presence of a cantilever pile wall only reduced rotation values to acceptable levels in cases involving soft clay, as stated by (C.-Y. Ou, 2014).

An approach based on elastic displacement theory is proposed to predict the settlement profile resulting from excavations. To address this, a closed-form method is utilized, leveraging the superposition technique to extend the fundamental solution from translation and wall deflection mode to the broader wall deflection mode. The displacement boundary of the problem is determined by assuming a piecewise quadratic function for the deflection of the wall in braced excavations. This approach leads to the creation of an explicit solution that is user-friendly and easy to implement (Fan et al., 2021). In a study conducted by (C.-Y. Ou & Shiau, 1998) three-dimensional finite-element analysis is presented for excavations. Traditional finite-element analysis typically demands significant computer storage and calculation time, requiring the boundary to be set at a sufficient distance from the excavation zone to achieve convergence. To address this, the researchers introduced the concept of infinite

elements into the three-dimensional finite-element computer program. By strategically placing infinite elements at one wall depth intervals, satisfactory convergence is achieved for wall deflection and ground surface settlement.

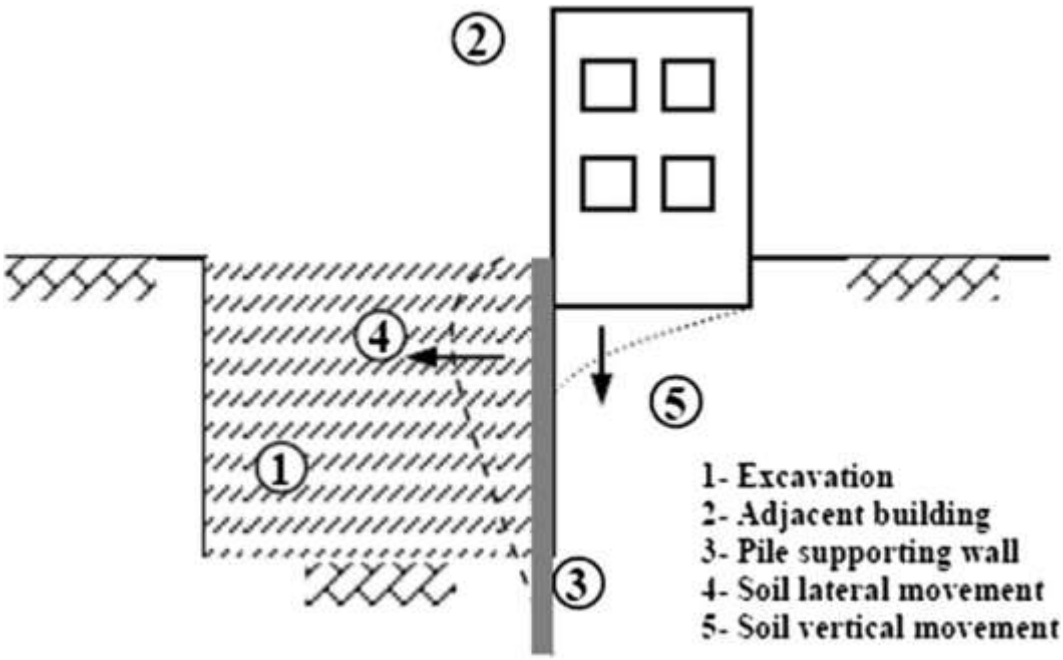

Figure 1-1: Model of Excavation, adjacent area and building (Ramadan et. al., 2018)

Piles are widely used to transfer vertical (axial) forces, which are principally caused by gravity (for example, the weight of a superstructure). The piles in all of these structures, however, are subjected to lateral (horizontal) forces and moments in addition to the axial force.

In fact, piles are used primarily to transfer lateral forces in in construction works like earth retaining structures. The primary purpose of piles in earth retaining structures is to resist the lateral stresses caused by the soil pressure exerted by the mass behind the retaining wall. In certain cases, piles are also installed in slopes experiencing gradual earth movements to counteract the displacement. In such scenarios, the piles experience primarily lateral forces. Open excavations are supported by piles; there is no axial force present, and the piles' main function is to withstand lateral forces.

1.2 Need of research

During the late Pliocene period through the Quaternary, the basin was filled with sediments of fluvio-lacustrine origin. The formations in the basin, listed in ascending order, are Dharmasthali, Kalimati, Gokarna, Thimi, Tokha, and Patan, as stated by Sakai et al. in 2001 and 2008. Patan, consists of fluvial layer ranging from 14,000 to 19,000 years (Paudayal, 2011) up to the last glacier, around 10,000 years ago. Gokarna formation began during the Middle Pleistocene. The Kalimati formation, which primarily comprises black organic clay, silts, sand, and gravel, is known as the "black mud" in Nepal. Its age ranges from 2.8 million years (late Pliocene) to 30 kyr (Pleistocene), and it is the only formation that extends across the central basin, as described by Maskey in 2019. The Engineering and Environmental Geological map of Kathmandu Valley indicates that the project site is situated in slightly consolidated sediment of Plio-Pleistocene age within the Kalimati Formation. The sediment consists of grey to dark silty clay and clayey silt, with some areas displaying calcareous properties and phosphate minerals. Organic clay, fine sand beds, and peat layers are commonly found. The project area is located in a hazardous zone with potential foundation instabilities and areas of low bearing capacity, where settlements can occur due to the presence of soft, silty clay, peat, and plastic clay beneath the soil cover. Special foundations are required for constructing buildings, and heavy construction necessitates protective measures. Therefore, the objective of this study is to investigate the behavior of soil-pile interaction under various loading conditions within the Kalimati Formation.

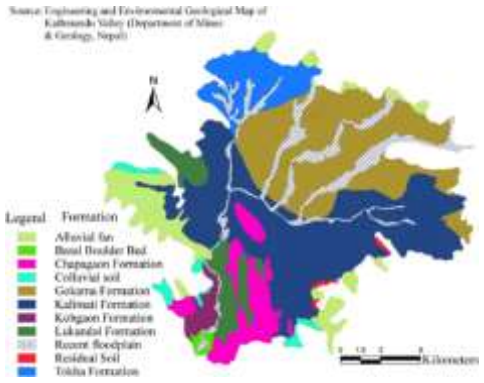

Figure 1-2 Engineering and environmental geological map of Kathmandu valley

1.3 Objectives

1.3.1 Global objective

The major goal of this study is to look into how different parameters affect the excavation support system.

1.3.2 Specific objective

- To study the effect of the adjacent building foundation type.
- To compare the behaviour of pile wall for excavation support in soft ground by using 2D and 3D FEM method.
- The specific objective of this thesis is to study deflection and bending moment performance behaviour with respect to:
    - Undrained shear strength
    - Depth of excavation
    - Stresses under foundation of the adjacent building
    - Pile embedment depth
    - Pile diameter

1.4 Research Motivation

In order to improve construction practices in the Kathmandu Valley, protection piles are frequently employed to support excavations in major construction developments such as large buildings and highway safety. They are also used to bear the additional load imposed by nearby existing structures. Consequently, the aim of this study is to investigate the response of laterally loaded piles in clayey soil within the Kathmandu Valley.

2 LITERATURE REVIEW

To enhance the understanding of the research work, a thorough review of recent and reliable literature relevant to the study was conducted. Various sources such as papers, books, journals, articles, and abstracts were examined to gather valuable insights.

2.1 Theoretical Aspects

Theoretical and empirical methodologies provide a fundamental understanding of deep excavation performance in a fundamentally new way. They do, however, have limitations due to their simplicity and assumptions. This section goes over a few of these methods.

2.1.1 The conventional earth pressure hypothesis

Active earth pressure must be evaluated when designing retaining walls, and this evaluation is mostly based on the traditional lateral earth pressure configurations described by Coulomb (1776) and (Rankine, 1857). The limit equilibrium method was first used to address the ground pressure problem by Coulomb (1776) who concentrated on the degree of stability of a soil split between a retaining wall and a failure plane. This approach is primarily applicable to frictional soils in the active state, rather than cohesive soils or passive conditions. It is assumed that the point of active thrust application is one-third of the wall's height from the base and is unaffected by things like soil friction angle, wall friction angle, backfill angle, and wall incline angle. Based on plastic equilibrium, (Rankine, 1857) developed a remedy for lateral earth pressures in retaining walls. He figured there wouldn't be any resistance between the dirt and the retaining wall, isotropic and homogeneous soil, uniform friction resistance on the failure surface, and a rectangular shape for both the failure and backfilled surfaces.

By directly integrating the balance equation on an integrated planar and logarithmic spiral failure surface, (Caquot & Kérisel, 1948) gave tables of active earth pressure coefficients. They considered friction between the retaining wall and the soil, as well as a curved failure surface that closely approximates the true failure surface. These active as well as passive coefficients can be used to assess over time in soils with

cohesiveness when entire pore water pressure release takes place, despite the fact that they were created for cohesion-free soils. Modern calculations of earth pressure are based on these historical conceptions of earth pressure and the developments that followed. However, they are only useful for a general estimation of ground forces on the wall under certain conditions. They also don't take construction into consideration and don't show signs of wall deflections or movement of the ground in more intricate braced deep excavations.

2.1.2 Analysis of Stability

The design of clay retaining walls must take stability examination into consideration, which is frequently done using limit equilibrium or finite element methods. Limit equilibrium methods are frequently used in design computations, which assume uniform distributions of active as well as passive earth pressures on both the front and the back of the structure and take into account moments near the prop's location. According to a method put forth by (Terzaghi, 1943) failure of the load-bearing capacity is caused by a soil column beyond the excavation, but is prevented by the weight of a comparable soil column inside the excavation and adhesion along the vertical margins. In order to evaluate basal heaving failure in deep excavations in soft clays, (Bjerrum & Eide, 1956) considered the base of the excavation as a negatively laden, entirely level foundation and gathered data on total or partial failure occurrences.

The calculated safety factor was discovered to be less than 1.0 in failure situations, slightly above 1.0 in partial failure cases, or not detected at all. The basal heave factor of safety estimated for an isotropic soil may underestimate the value of the safety factor for an anisotropic soil, according to (Clough & Hansen, 1981), considered the anisotropy of clay strength within the factor of safety proposed by with the effect becoming more pronounced as the extent of anisotropy rises. This was suggested when considering the anisotropy of clay strength within the factor of safety proposed by (Terzaghi, 1943). (O'rourke, 1993) altered the equations for basal stability to take wall flexure into account below the excavation stage. The buried wall depth was considered to have no bearing on the geometry of the basal failure mechanism. However, a rise in stability was anticipated because of the retained strain energy in flexure. As a result,

stability factors were generated that were reliant on the yield moment and the presumptive boundary parameters at the wall's base.

2.1.3 The Stress Path Method

The behavior of soil is influenced by both the existing stress conditions and the stress history it has experienced. It is less stressful on the soil within the excavation when it is excavated deeply, and the soil on the retained side is no longer constrained on the lateral plane. It is crucial to understand the stress path that occurs in the field during the excavation process. As the stress condition of the soil affects excavation behavior, this understanding aids in identifying the fundamental variables impacting shear strength and determining acceptable stiffness as well as strength characteristics from experimentation for design and analysis. The stress path methodology offers a helpful way to understand the various functional pressures in soil components at typical sites, which are brought on by the combination of vertical and horizontal stress reduction throughout excavation.

In a deep excavation, (Ng & Yan, 1999) compared actual stress paths along a diaphragm wall to pertinent experimental triaxial stress path results. They discovered that the stress channels in the field that are successful in front of the wall closely reflect the stress paths in the lab that are seen in undrained extended testing. The effective stress routes in the field, however, did not match up well with those discovered during laboratory undrained compression testing. The soil at the soil-wall interface may have previously reached or been close to reaching the active condition due to the large horizontal stress reduction experienced during wall building. Soil directly beyond a wall during fairly quick excavations in clay that is stiff may deviate from the typical notion of undrained behavior.

In order to explore the development of lateral ground pressure on well-braced diaphragm structures in deeper soil excavating and to comprehend the process of soil arching, (Hashash & Whittle, 2002) used nonlinear finite element analysis. At the highest level of excavation, the soil in the direction of the wall experiences stress along a typical plane strain inactive shear pattern. However, because of the rotation of the primary stress axes and the inversion of the shear direction brought on by the soil

arching mechanism, the soil components beyond the structure on the maintained side exhibit more complicated pressure courses.

2.2 Empirical Observation

According to the soil type and construction methods used, (Peck, 1969) divided the motion of the settlement graph into three distinct regions after conducting an extensive analysis of excavations all over the world. The estimation of ground-level settlements using this method has been done in a variety of settings. Whereas important elements like the soil composition, the technique used to place the walls, the type of retaining wall, and the order in which the construction was done are all ignored in the generic description of the settlement curve. Those instances are also older than 1969 and use flexible sheet pilings or soldier pile with lagging, that cause far larger movement of the ground than tougher diaphragm walls built from the top down. As a result, using this scientific approach to forecast ground movements in a particular deep excavation project is difficult. (Clough, 1990) suggested that the settlement pattern for excavations in sandy deposits or clay that is stiff takes the form of a triangle shape, with the largest settlement taking place along the wall. The corresponding settlement for sandy soil and rigid to extremely hard clays, according to non-dimensional identities, spreads out to about 2 and 3 times the depth of the excavation, respectively. A trapezoidal-shaped settlement trench was proposed because in soft to medium clay, the greatest amount of settlements happens some distance from the wall. Up to twice as deep as the excavation, the affected area may exist.

According to field data, (Terzaghi, 1943) proposed that the earth pressure, on average, remains relatively constant as you go deeper, with slight reductions at the top and bottom of the wall. (Terzaghi et al., 1996) suggested using apparent earth pressure envelopes to estimate the maximum loads on struts in a braced excavation based on field observations from different sites. These figures, however, fail to accurately reflect the real variation in ground forces at certain vertically excavation segments. Several academics have critically analyzed this strategy, including (Poh & Wong, 1998) and (Hashash & Whittle, 2002).

(Mana & Clough, 1981) related the standardized peak recorded wall motions across the excavation level to (Terzaghi, 1943) measure of safety factor over basal heave based on analyses of various case histories in soft to medium clays. While sudden increases in variations at a smaller factor of safety imply subsurface yielding, consistent non-dimensional displacement at a greater factor of safety implies a mostly elastic reaction.

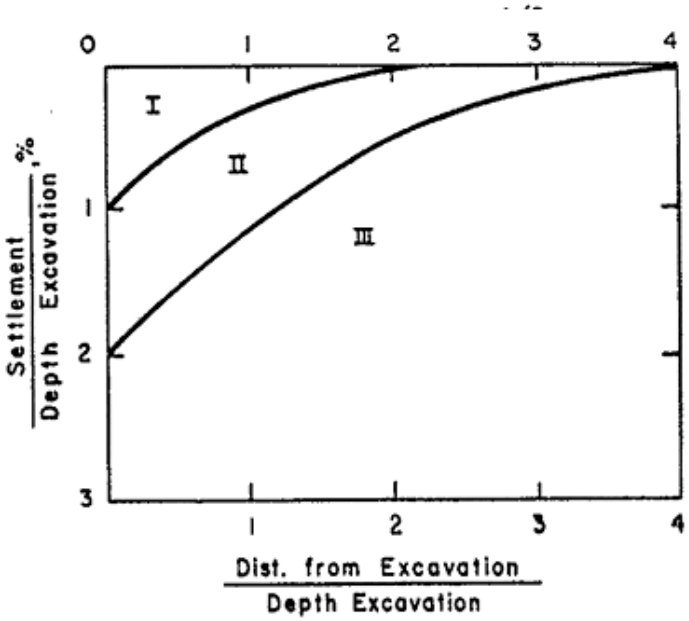

I- Sand and Soft to Hard Clay, Avg. Workmanship

II- Very Soft to Soft Clay
1. Limited Depth of Clay Below Bott. Exc.
2. Significant Depth of Clay Below Bott. Exc., But $N_b < N_{cb}$*

III- Very Soft to Soft Clay to a Significant Depth Below Exc. Bott. and $N_b > N_{cb}$

* N_b = Stability No. Using C "Below Base Level" = $\frac{\gamma H}{C_b}$
N_{cb} = Critical Stab No. for Basal Heave

Figure 2-1 Graph showing ground settlement near excavations in different soils as a function of distance from edge.

An approach was proposed to forecast the anticipated movement of walls by establishing upper and lower bounds. (Wong & Broms, 1989) introduced an initial method to assess the lateral deflection of sheet-pile walls that are either strutted or anchored, ranging from ordinary to exceptional quality, in clay. The strategy implies

that the structures are flexible and that their lateral deformations are controlled by the soil's plastic yielding at the excavation's bottom. There are no net volume changes during the excavation, and the volumes related to earth's settlements are equivalent to those related to heave and lateral movement of the wall above the bottom of the excavation. The depth, width, and secant or tangential modulus of the soil in the excavation are all taken into consideration throughout the study. (Clough et al., 1989) suggested a semi-empirical approach to calculate wall displacement brought on by clay excavating. (Terzaghi, 1943) assesses the wall's maximum horizontal movement in relation to the system stiffness and the basal heave safety factor. The generated curves are based on typical circumstances, high standards, and the presumption that only a tiny amount of the movement is caused by the wall's cantilever distortion.

(Hsieh & Ou, 1998) proposed a classification system for ground settlement profiles, distinguishing between spandrel and concave profiles. They developed an experimental technique to predict these settlement profiles by analyzing field observations through regression analysis. To determine the greatest deflection of a wall and the ground level settlement brought on by a braced excavation in soft to medium clays, (Kung et al., 2007) developed a semi-empirical model. A database of 33 case studies and in-depth finite element analyses were used to construct the modelIt is made up of three main parts: the maximum horizontal wall deformation, the proportion of the maximum ground-level settlement and the maximum horizontal wall deformation, and the ground surface settlement profile. The largest wall deformation and the deformation ratio, among other possible input variables, were used to create the correlations between the input variables using regression-based equations. After a bias analysis, it was determined that the model's precision was enough for real-world use. Using histories of cases that weren't used when the model was being developed, the suggested model was validated.

2.2.1 Basal Stability

To analyze the basal stability of deep excavations, limit equilibrium methods are widely used. (Terzaghi, 1943) hypothesized a failure mechanism, which is depicted in Fig. 2.1. This mechanism is the same as the bearing capacity failure mechanism. Based on the

findings of (Bjerrum & Eide, 1956), Terzaghi's approach is considered dependable for homogeneous soil with excavation depth B H. However, it may not be reliable for narrow excavations (B H) or when there is a stiff dried crust present on the surface. Bjerrum and Eide proposed an alternative concept called the inverted bearing capacity, where they likened the unloading effects caused by excavation to the upward loading experienced by a building foundation. They applied the bearing capacity equation for deep foundations to calculate the ultimate unloading pressure.

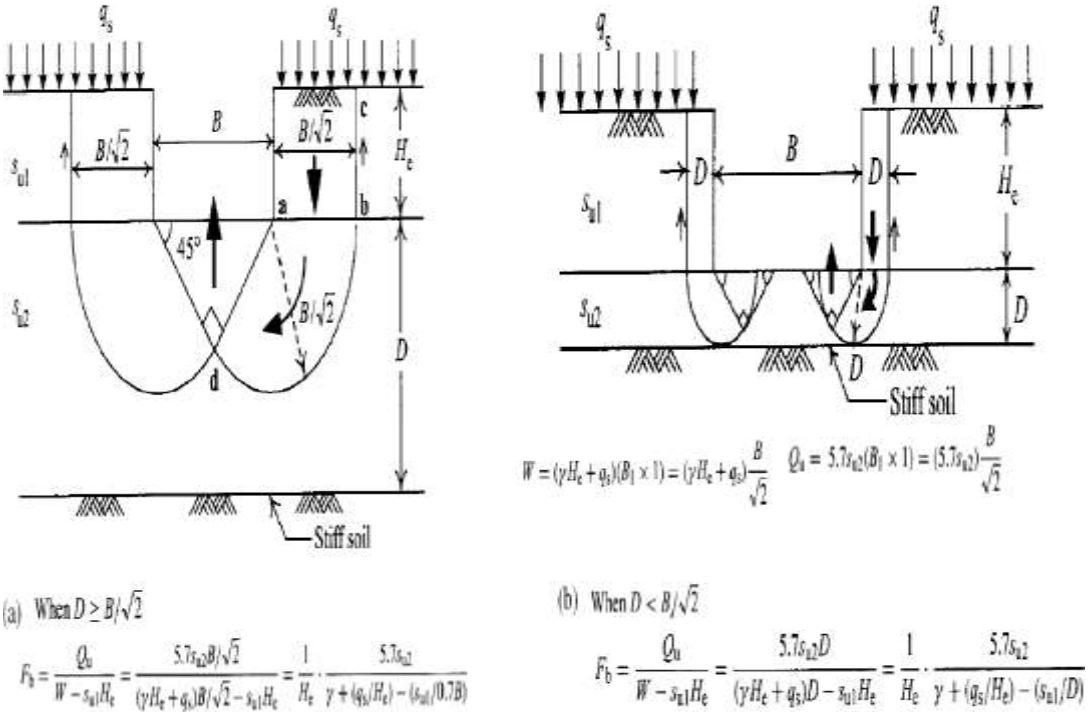

Figure 2-2 Basal Stability- Terzaghi Method

(Mana & Clough, 1981) documented examples in which the factor of safety calculated using Terzaghi's approach was less than unity, but the excavations did not collapse. According to the findings of this study, Terzaghi's technique may be cautious in certain scenarios. (Hashash & Whittle, 1996) compiled a list of various approaches for calculating the safety factor to basal heave. They determined that the penetration depth of the support wall has a major impact on the overall stability of the excavation and that the presence of the wall limits soil failure (unless structural failure of the wall occurs).

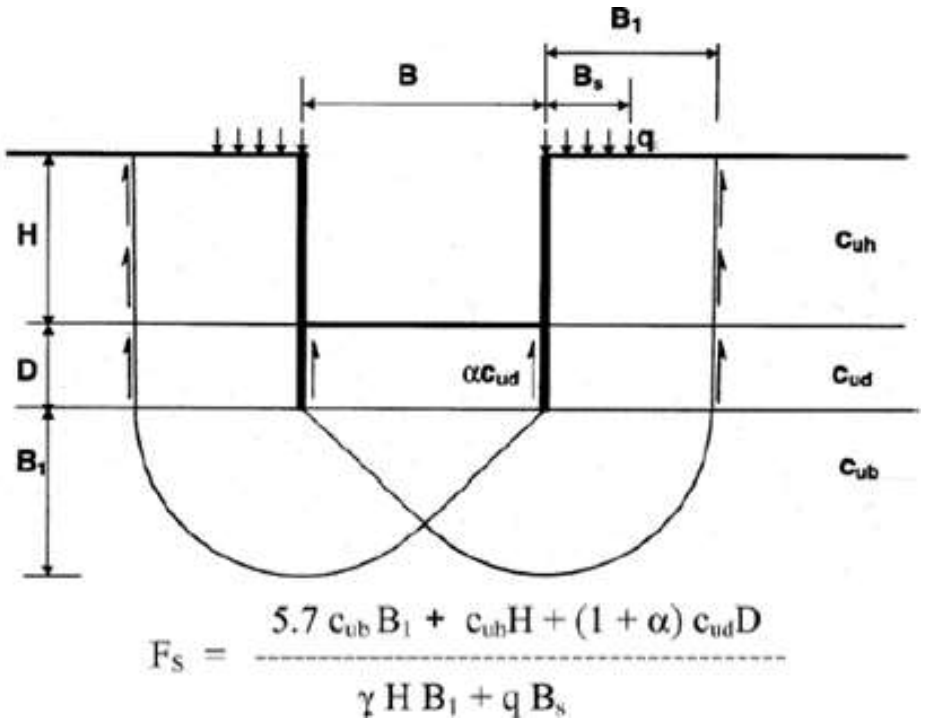

Figure 2-3 Modified Terzaghi Method (Wong and Goh, 2002)

Terzaghi's method was modified by Wong and Goh (2002) by taking into account the impact of hard wall penetration below the bottom of the excavating, as shown inFigure 2-3. They showed how the safety factor found using the modified approach closely matches two particular situations. According to (C. Y. Ou et al., 2006), Terzaghi's original estimation of basal heave is not influenced by the presence of a retaining wall. But adding a strong wall for retention ought to raise the level of safety. In other words, the real safety factor should be higher than the one anticipated by Terzaghi's technique given the existence of the stiff supporting structure. The study also showed that several assumptions in Terzaghi's technique, such as the failure surface reaching the level of the ground and full mobilization of shear strength across the failure surface, prevent it from consistently producing appropriate results. Deeper excavation don't always support these presumptions. The approach developed by Bjerrum and Eides, in contrast, took into account a number of variables, such as the depth, width, and form of the excavation, making it relevant to a variety of deep and shallow excavation shapes.

2.3 Piled Retaining Walls

Column piles, sometimes referred to as in-situ pile walls of retention, are made up of rows of piles made of concrete that are built either using the cast-in-place pile method or the precast pile method. Compared to soldier piles or sheet piles, column piles have the advantage of generating less noise and vibration. They are also more rigid, providing better control over ground movements and minimizing the need for extensive bulk excavation. There are three main types of bored pile walls commonly used: contiguous walls, secant walls. Construction of continuous pile walls leaves few spaces in between the piles. In this method, successive unconnected piles are drilled utilizing affordable augers, such as Contiguous Flight Auger (CFA) rigs. The diameter and spacing of the piles depend on factors such as the soil type, groundwater level, and design forces. It is important to avoid large spacing between piles to prevent soil collapse through gaps. The diameter of CFA piles typically ranges from 300mm to 1000mm. In small to medium-scale excavations, CFA piles are considered more cost-effective than diaphragm walls in terms of both cost and time savings. Additionally, the use of bentonite mud for excavation is not required with CFA piles.

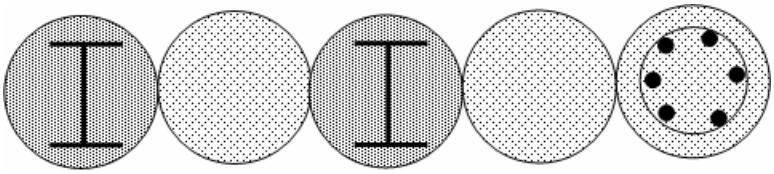

Figure 2-4 Tangent Pile Wall

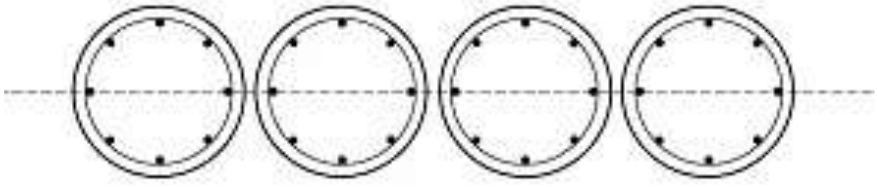

Figure 2-5 Contiguous Pile Wall

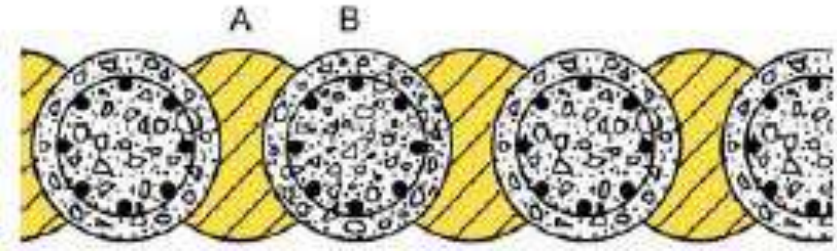

Figure 2-6 Secant Pile Wall

Contiguous piles assist restrict movement of the ground on the backfill side, making them an appropriate choice in highly populated metropolitan locations where traditional retaining techniques might encroach on neighboring properties. The pile construction involves drilling a Contiguous Flight Auger (CFA) into the ground. Cement-sand grout or concrete is pumped under high pressure via the hollow shaft as the auger is removed. In order to facilitate extraction and provide lateral pressure to the nearby soils, the grout or concrete pressure remains constant through removal. A reinforcement cage is then put into the liquid column of grout or concrete when this procedure is finished. Cost and time savings can be achieved when CFA piles are used in conjunction with capping beams or breasting beams, which help distribute pressure in the piles. Additional facing is often added for aesthetic purposes. CFA piles can be utilized in various soil conditions, including granular soils, cohesive soils, and soft rocks. However, they are unsuitable for soft clays, weak organic soils, and hard rocks. Contiguous walls can only be used when there is no risk of groundwater, unless grouting or jet grouting is employed to address leaks between the piles. Water can accumulate and be discharged near the base of the wall. Capping beams at the top to aid in the distribution of pressure in piles. Separate facing is typically provided to improve appearance. CFA piles can be employed in a variety of soil conditions, including granular soils, cohesive soils, and soft rocks. Due to wall bulging, soft clays and weak organic soils are inappropriate. Additionally ineligible are hard rocks. Only areas with no risk of ground water or those where leaks between piles can be fixed using grouting or jet grouting may use the contiguous wall. However, a sufficient volume of water can be gathered and pushed out near the base. The gaps between piles and the ensuing issues of lack of water proofness, which were the fundamental

challenges of contiguous pile walls, have been successfully overcome by interlocking or secant piles.

Secant pile walls are constructed using intersecting piles with spacing less than the diameter of the piles. These walls are used to create cutoff walls, restricting groundwater inflow and reducing movement in weak and moist soils. Secant walls can be categorized as either hard/firm or hard/soft, or they can also be characterized as hard/hard. For hard/soft or hard/firm secant walls, the space between the primary piles (A) is occupied by using a weaker mix of concrete for hard/soft walls and an unreinforced cement/bentonite mixture for hard/firm wallsThe installation of the primary piles is done first, and then the secondary piles (B) are built by cutting accross the primary piles with reinforced concrete. The diameter of these piles typically ranges from 500mm to 1200mm. The main piles (A) in hard/hard secant walls are constructed of extremely strong concrete and may be strengthened further. The secondary piles (B) are cut into the concrete primary piles (A) using specially made cutting heads on heavy-duty piling rigs. Tangent pile walls, on the other hand, consist of drilled shafts placed in close proximity so that they touch each other. In general, secant pile walls are more successful in preventing groundwater intrusion in excavations than tangent pile walls because they are stiffer (Godavarthi et al., 2011).

2.4 Load Transfer Mechanism (Statics) of Piles

To properly study and design piles, it is crucial to have a comprehensive understanding of the mechanisms involved in transferring axial and lateral loads. When it comes to axial (vertical) loads, piles can be likened to vertically loaded columns that transmit loads to the ground through two main mechanisms: shaft friction and base resistance (as shown in Figure 1.1). When subjected to axial loads, a pile experiences slight settlement while the surrounding soil resists the downward movement. Because of the soil's friction characteristics, the interface among the shaft of the pile and the soil that surrounds it produces frictional forces, which prevent the pile from descending. The applied axial force is partially resisted by these frictional forces along the pile shaft, sometimes referred to as shaft resistance. In addition, a portion of the axial force is transferred to the ground's surface via the pile base, which is the bottom of the pile.

When the pile tries to settle, the earth beneath it offers compressive resistance, sometimes referred to as base resistance or end-bearing resistance. The overall resistance, comprising shaft friction and end-bearing resistance, maintains the pile's equilibrium under load. End-bearing piles primarily carry the axial load through the base, while friction piles transfer the load predominantly through shaft friction. End-bearing piles must be positioned in a solid soil layer, such as one made of hard rock, stiff clay, or deep sand. Engineers generally prefer end-bearing piles as they provide more reliable base resistance compared to shaft friction. Engineers must only rely on shaft friction if a strong soil layer is absent; in this scenario, the pile is referred to as floating pile.

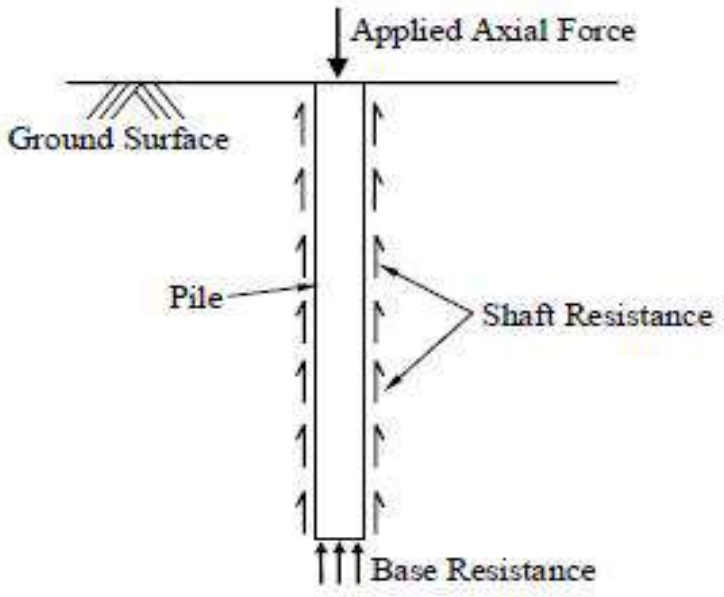

Figure 2-7: Mechanism for Axially Loaded Piles to Transfer Load

Pile behavior under lateral loads is similar to that of transversely loaded beams. To transfer lateral weight to the surrounding soil mass, they make use of the lateral resistance of the soil Figure 2-7. When a pile is loaded laterally, some or all of it tries to move horizontally in the direction of the applied weight, bending, rotating, or translating the pile. The pile causes compressive and shear stresses and strains in the soil, which function as a barrier to pile movement. The pile presses against the soil in front of it (i.e., the soil mass laying in the direction of the applied force). For lateral

loads, this is the principal load transmission mechanism. The external horizontal forces are balanced by the total soil resistance operating throughout the entire pile shaft. The soil resistance also permits the pile's moment equilibrium to be satisfied.(Fang, 2013)

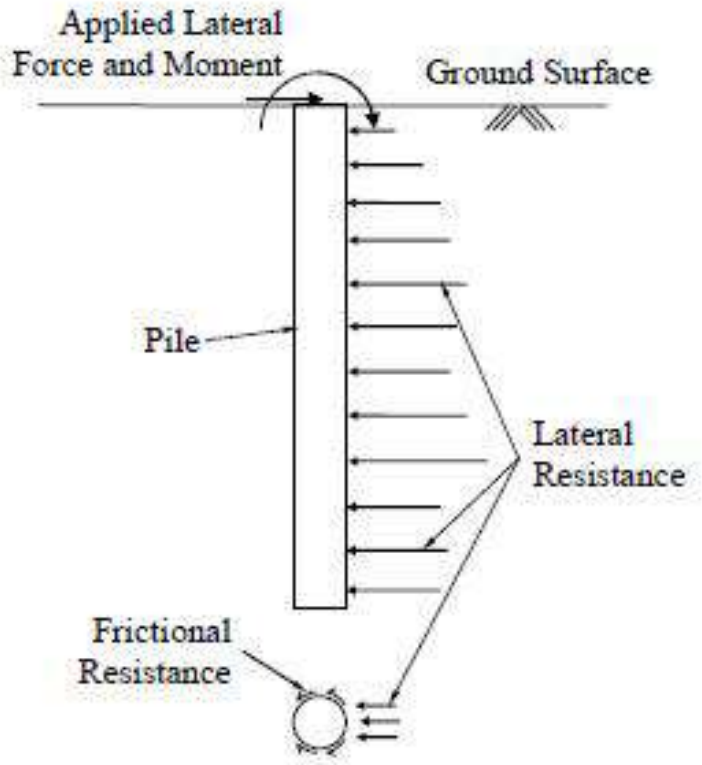

Figure 2-8: Load transfer behavior of Laterally loaded single pile

2.5 Laterally loaded pile behavior and failure modes

Axially loaded piles behave in a fairly predictable way: in reaction to the applied load, the pile descends vertically. The pile may endure severe vertical deflection (plunging) and eventually fail if the resistance actions, such as shaft and base resistances, are at their maximum. However, depending on the type of pile, laterally laden piles display more intricate kinematics and failure processes. These piles can undergo spinning, flexing, or translation due to the transverse load application. Especially in the top few meters, a gap may appear between the rear of the pile and the neighboring earth as the laterally laden pile travels in the direction of the force that is applied. The specific behavior and failure modes of laterally loaded piles are influenced by various factors and require a more detailed analysis Short and stubby piles are known as inflexible

piles since they can rotate and possibly shift but won't bend very much as shown in Figure 2-9. Because of the imposed load, the pile bends if it is long and skinny Figure 2-10., they are called flexible piles. Typically, piles are sufficiently long to function like movable piles. The laterally loaded pile issue is a relationship between soil and structure problem using flexible piles, where the soil resistance is affected by the pile displacement and vice versa.

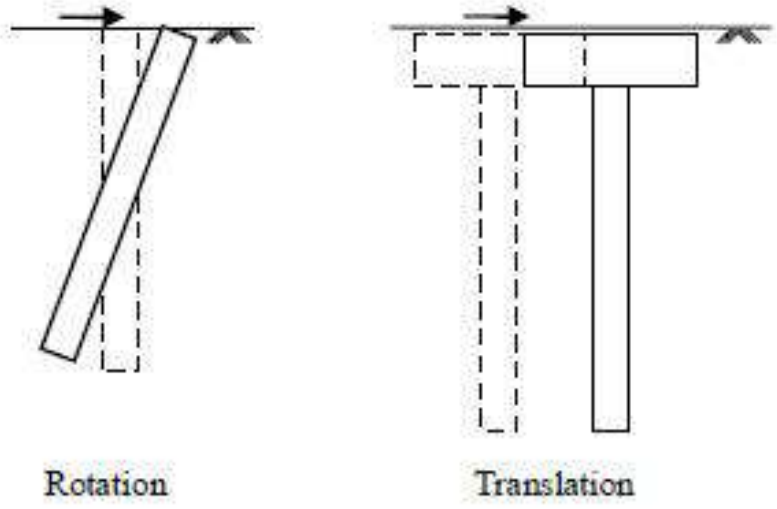

Figure 2-9: Short pile failure mechanisms (Rishitha, 2015)

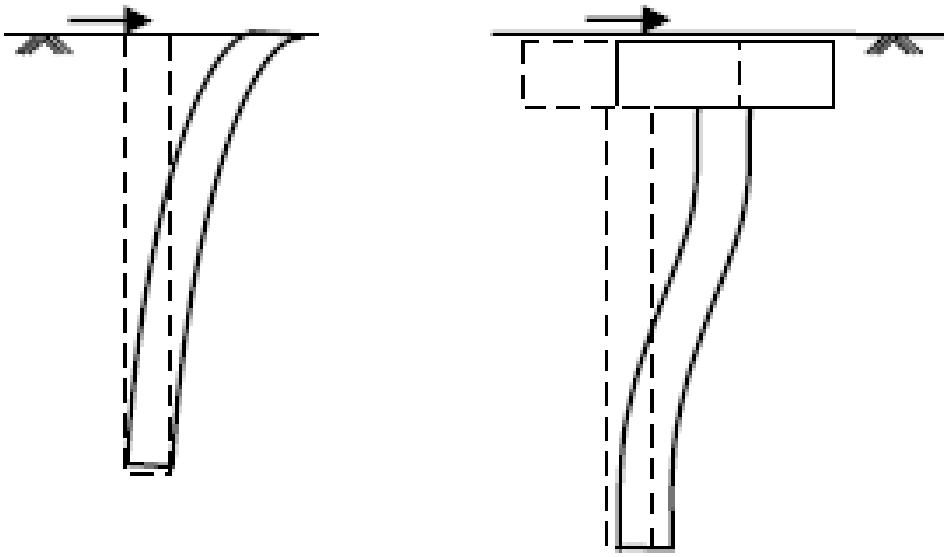

Figure 2-10: Long piles failure mechanisms (Rishitha, 2015)

2.6 IS Code Method

2.6.1 Background

The IS code approach substitutes a cantilevered structure for the pile, which remains stationary at a specific depth and disregards the soil supporting over that level. The length of which is determined by the surrounding soil's subgrade reaction and the pile geometry. As shown in Figure 2-11, corresponding cantilevered distance Le = L_1+L_f, where L_1 the height of the pile above the level of the ground and L_f is determined as a function of (L_1/T or L_1/R). However, the procedure described here is only applicable to flexible piles with a highest depth factor L/T of 4.0 or greater. Choosing whether the pile will be a finitely long flexible part or a brief stiff unit is the first step. This is achieved by figuring out if the object has a stiffness value of R or T. Choosing either the pile is going to be a finitely longer elastic part or a brief stiff unit is the first step. To do this, the stiffness factor R or T for the particular pile and soil combination must be calculated. Once the stiffness factor has been calculated, the embedded measurement L of the pile is coupled to the requirements for behavior as a shorter stiff pile or as a long flexible pile. Then, using conventional elastic analysis, the distance below the level of the ground to the location of virtual fixation is calculated, and the lateral deflection and bending moment are estimated.

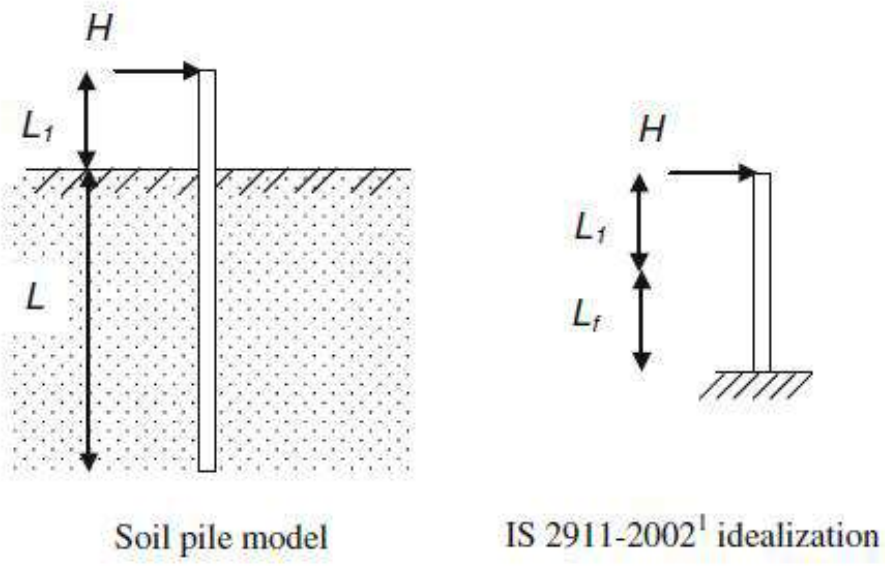

Figure 2-11: Cantilever modelling of laterally loaded pile (IDS 2911 (Part / Sec1), 2010)

For Sand-Based Piles and Normally Loaded Clays

Factor of stiffness:

$$T = \sqrt[5]{\frac{EI}{\eta_h}} \ (in\ m)$$

here E = Materials' Young's modulus in MN/m^2

I = Cross-sectional M.I of the pile in m^4

η_h = Subgrade reaction modulus in MN/m3. Table 2-1 lists the range of h for different sand kinds that are categorized based on the SPT number for both dry and submerged sand circumstances.

Table 2-1: Granular soils' Modulus of Subgrade Reaction

Sl.no	Soil type	N (blows/30cm)	Range of η_h (MN/m^3)	
			Dry	Submerged
1.	Very Loose sand	0-4	<0.4	<0.2
2.	Loose sand	4-10	0.4-2.5	0.2-1.4
3.	Medium sand	10-35	2.5-7.5	1.4-5.0
4.	Dense sand	>35	7.5-20.0	5.0-12.0

In regards to piles in preloaded clays:

Stiffness factor

$$R = \sqrt[4]{\frac{EI}{KB}} \ (in\ m)$$

E = Materials' Young's modulus in MN/m2
I = Cross-sectional M.I of the pile in m4

$$K = \frac{K_1 * 0.3}{1.5 * B}$$

B = Pile width or diameter in meters

The range of subgrade response modulus for several types of clays that are categorized based on unconfined compressive strength is provided in Table 2-2.

Table 2-2: Cohesive soil's modulus of subgrade reaction, k_1

Sl.no	Soil Consistency	Unconfined Compressive Strength (kN/m^2)	Range of k_1 (MN/m^3)
1.	Soft	25-50	4.5-9.0
2.	Medium stiff	50-100	9.0-18.0
3.	Stiff	100-200	18.0-36.0
4.	Very stiff	200-400	36.0-72.0
5.	Hard	>400	>72

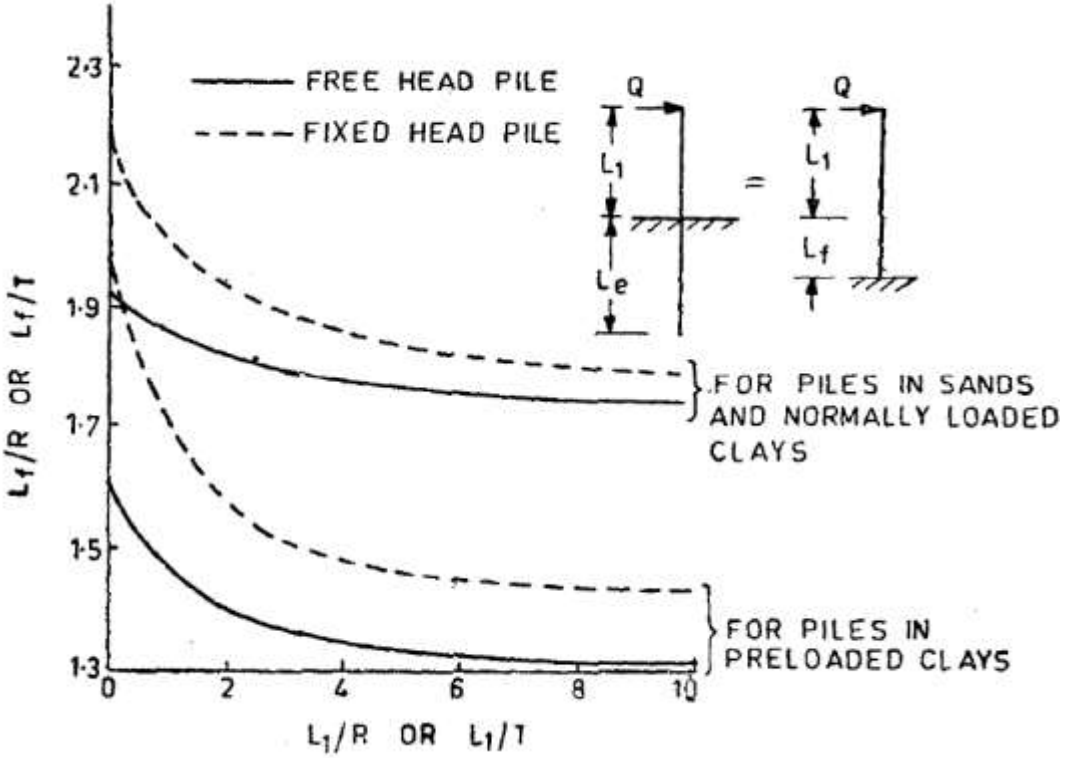

Figure 2-12: Depth of Fixity (Is2911 (Part 1/Sec 1), 2010)

2.7 Deflection and Moments

The equivalent cantilever methodology provides a straightforward method for calculating displacement and moments owing to minor horizontal force. This necessitates the estimation of virtual fixity z_f depth. The charts in Fig. 8 can be used to calculate the depth to the point of fixity. Either by converting the moment to an equivalent lateral force or by measuring the actual position of the lateral load applying,

one can determine the effective eccentricity of the point of load application, or e. The two stiffness variables described above are R and T.

For a free head pile Deflection $Y = \frac{H(e+z_f)^3}{3EI} * 10^3$

and for a fixed head pile deflection, $Y = \frac{H(e+z_f)^3}{12EI} * 10^3$

The corresponding cantilever's fixed end moment is bigger than the pile's real peak moment (M). The corresponding cantilever's fixed end moment has been multiplied by a reduction factor, m, to get the actual maximum moment. The following equation can be used to get the corresponding cantilever's fixed end moment:

$$M_F = H(e + z_f)\ Free\ head\ pile$$
$$M_f = \frac{H(e+z_f)}{2}\ \ Fixed\ head\ pile$$

The true peak moment (M) = m M_f

Where 'm' is reduction factor that is found from Fig 2.3 for a free head pile and from Fig 8. For a fixed head pile.

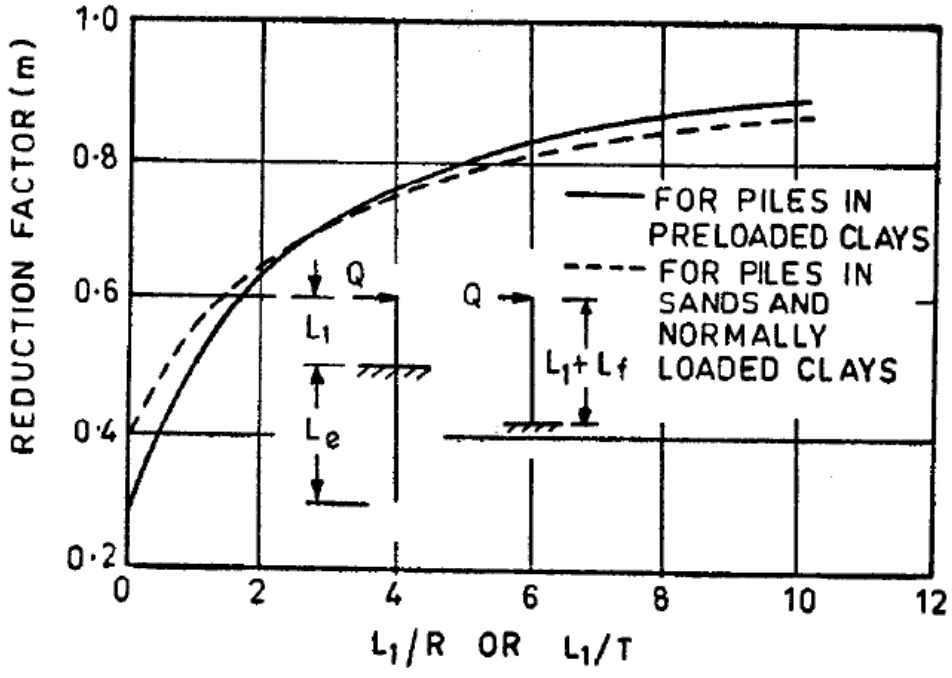

Figure 2-13: Free head pile reduction considerations (IS 2911 (Part 1/Sec 1), 2010)

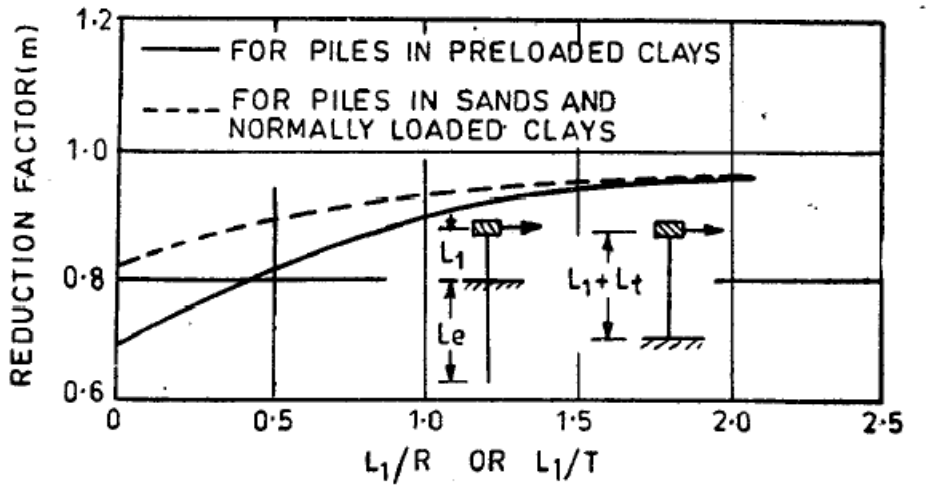

Figure 2-14: fixed head pile reduction considerations (IS 2911 (Part 1/ Sec 1), 2010)

2.8 A summary of Previous Research on Laterally Loaded Piles

In this section, we present a concise overview of the commonly used analytical methods. The performance of closely separated piles or groups of piles can be estimated using these strategies. The four sets of computational methods for estimating lateral deflections, shifts, and pressures in specific piles are as follows:

- Winkler strategy,
- p-y method,
- The elastic theory, and
- Finite element procedures

2.9 Numerical Modeling

A useful technique for examining the interaction of soil and structure in deeper excavations is numerical modeling, which can also supply all the information required for design. This section gives a brief summary of the early findings along with a portion of the numerical modeling methods that were used.

2.9.1 Model specifics and the simulation technique

Due to limitations in software and computational resources, 2D simulations, such as plain strain and axisymmetric analysis, have commonly been used to estimate the behavior of deep excavations in both design and research (Clarke & Wroth, 1984), (Hubbard et al., 1984), (Fourie & Potts, 1989), (Finno et al., 1991), (Powrie & Li,

1991), Simpson 1992, (Hashash & Whittle, 2002). However, it is important to recognize the limitations of 2D analysis and consider fully 3D investigations when necessary. For instance, corner effects found in deep excavations, where movement of the ground and wall displacement are less pronounced near the wall corners than the wall the center spot cannot be explained by 2D analysis. Comparing 2D plane strain study to a streamlined 3D symmetrical squared or a rectangle analysis also tends to overstate wall displacement and soil settlements beyond the wall (C.-Y. Ou et al., 1996), (Lee et al., 1998). The accuracy of the study is influenced by a number of variables, including excavation geometry, length-to-depth ratio, retaining wall stiffness, excavation dimension, soil qualities, and other pertinent variables. In addressing the challenges associated with modeling retaining structures in 3D finite element analysis, (Zdravkovic et al., 2005) contrasted the outcomes with comparable axisymmetric and simple strain simulations. The axisymmetric analysis and the 3D study exhibited better agreement, but the plain strain analysis produced superior forecasts of wall displacement diversion and ground displacement. The retaining wall was modeled using both shell components and active components, and it was discovered that wall deflection becomes greater when represented using shell elements because shear stresses generated on the rear of the wall are not there to provide a favorable influence. It was discovered that wall displacement and bending moment at the wall border are much higher than those obtained using the isotropic wall approach when the anisotropic wall technique was used to examine retaining wall discontinuities. The analysis focused on rectangular excavations, and 3D effects were observed. Although variations in wall depth were investigated, the impact on advancements and required forces was found to be minor.

Recent advancements in hardware and software have made it possible to employ fully 3D investigations for deep excavations, allowing for a more comprehensive consideration of geotechnical and structural details. The ground characteristics, excavation geometry, supporting framework, and constructing order are included in these specifics. This method can now be used to undertake extensive case studies. ((Hou et al., 2009), (Dong et al., 2013)). In order to thoroughly evaluate two distinct case studies—the long trench excavation of the Nicoll Highway Station and the

interaction between excavation and piling in the Common Services Tunnel. (Lee et al., 2011), and colleagues extensively used 3D finite element simulation. In their analyses, they accurately represented the geometry and arrangement of various retaining structures, including diaphragm walls, sheet pile walls. The outcomes of these studies were promising, and the field estimates obtained were reasonable, considering the inherent vulnerabilities and complexities associated with such assessments.

Recent advancements in computer technology have made it feasible to perform 3D analyses that take into consideration the impacts of excavation length and secondary walls spanning the extreme ends of the excavation. This is significant since earlier studies suggested that the absence of these parameters in plane strain evaluation made it difficult to anticipate excavation behavior. A 3D back-analysis of the installation chronology of the Lion Yard retaining wall by (Ng & Yan, 1999) revealed substantial stress transfer procedures and ground modifications. (Zdravkovic et al., 2005) addressed modeling concern regarding retaining structures in 3D finite element analyses, providing a comprehensive evaluation of ground and wall motions as well as wall's structural forces under various model suppositions.

(Finno et al., 2007)) investigated the length of the excavation has an impact on reinforced constructions in soft clay above medium and stiff clay using a parametric 3D finite element analysis. (Arai et al., 2008) analyzed using a 3D total stress elasto-plastic finite element analysis, the authors examined ground motions and stresses related to circular diaphragm walls and excavation of soil inside the walls. (Hsieh et al., 2013) conducted 3D numerical evaluations of four different deep excavation scenarios with varying cross wall mounting, demonstrating the effectiveness of cross walls in reducing lateral wall displacement. These studies highlight the value of employing 3D analyses to better understand the behavior of excavations and the impact of different factors on structural performance and ground response. (Orazalin et al., 2015) conducted 3D evaluations of the excavating support structure for the Stata Center Basement on the MIT Campus, emphasizing the significance of 3D excavation and support geometry on wall and ground movement. However, it should be noted that conducting a three-dimensional finite element analysis requires additional processing

time, making it less cost-effective in the industry. Therefore, it is important to determine when it is necessary to perform a three-dimensional analysis and when plane strain analyses can provide reliable data. This investigation aims to identify the circumstances where the benefits of a three-dimensional analysis outweigh the associated costs, while considering the industry's preference for more cost-effective plane strain analyses.

2.10 Mohr Coulomb Soil Model

When exposed to stress or strain, soils exhibit non-linear behavior. In reality, soil stiffness is determined by the amount of stress, the stress path, and the strain level. PLAXIS' sophisticated soil models incorporate some of these features. The Mohr-Coulomb model, on the other hand, is a well-known model of soil behavior that is linear elastic and totally plastic, can be utilized as a first approximation. linear elastic properties. Hooke's law of isotropic elasticity is used in part of the Mohr-Coulomb model. The Mohr-Coulomb failure criterion, which was created by Mohr and Coulomb in a plasticity framework with no linked plasticity, forms the foundation of the perfectly plastic component. When irreversible stressors occur, that is what is meant by plasticity. To determine if plasticity exists in a computation, a yield function, f, is included as an expression of stress and strain. The condition f = 0 is linked to plastic yielding. In main stress space, this state is frequently represented as a surface. A generative model with a set yielding surface—i.e., a yield surface wholly determined by model parameters and unaffected by (plastic) straining—is referred to as a perfectly-plastic model. The behavior is entirely elastic for stress states given by points within the yield surface, and all strains are reversible.

The MC model integrates linear isotropic elasticity, Hooke's law, and an extended version of Coulomb's failure criterion within an elastic perfectly-plastic framework. According to this concept, earth behaves as a linear elastic-perfectly plastic material by conforming to the Mohr-Coulomb yield surface. The model's failure criterion is displayed in The specifics of these factors are outlined in the following sections.

Table 2-3 and can be phrased as follows:

$$\tau_f = \sigma'_{nf} + tan\phi' + c'$$

In the context of the failure plane, τ_f represents the shear stress and σ′nf represents the normal effective stress. The plastic model parameters ∅′ and c′ correspond to the friction angle and cohesion, respectively, in Coulomb's failure criteria. In terms of effective primary stress, the Mohr-Coulomb yield function is defined as follows:

$$f = \frac{1}{2}(\sigma'_1 - \sigma'_3) + (\sigma'_1 + \sigma'_3)\sin\phi' + c'\cos\phi'$$

Here, σ'_1 and σ'_3 are, respectively, the primary stresses that are effective on the major and minor levels.

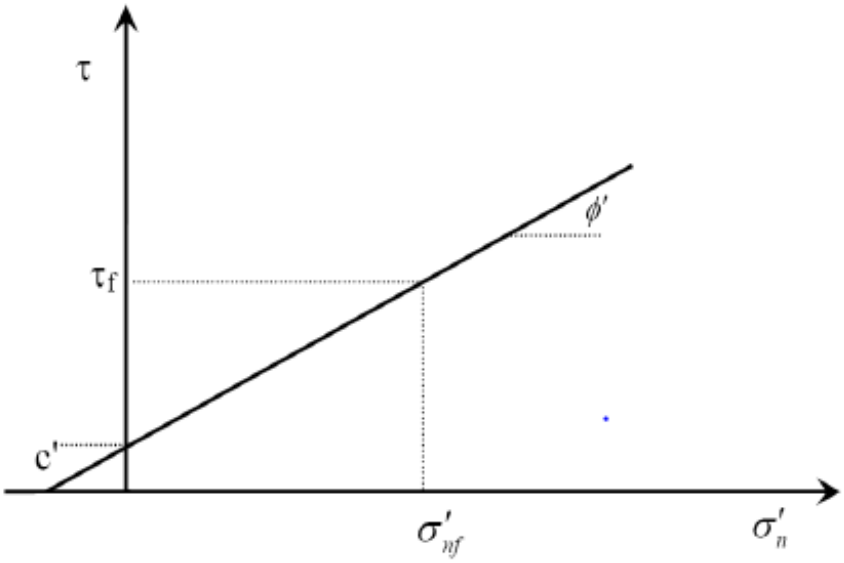

Figure 2-15: Failure Criterion of Mohr-Coulomb

Whenever it is described in terms of primary stresses, the complete Mohr-Coulomb yield condition comprises six yield functions, as described by Smith and Griffith (2013). In the primary stress space, this condition can be seen as a hexagonal cone as seen in Figure 2-16

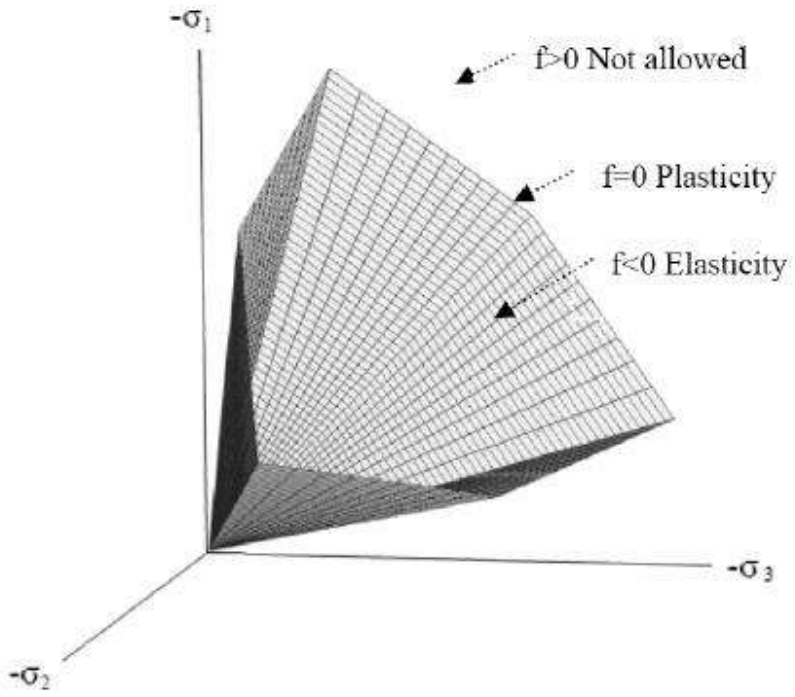

Figure 2-16: Mohr-Coulomb Yield Surface in Principal Stress Space (c'=0)

A dilatancy angle is added to Hooke's law and Coulomb's failure criterion in the MC model to account for the irreversible change in volume brought on by shearing. This inclusion makes the non-associated flow regulation representation more accurate. The MC model relies on a total of five parameters, which are listed in Table Table 2.3. The specifics of these factors are outlined in the following sections.

Table 2-3: Five required parameter for modeling

Parameter	**Description**	**Parameter evaluation**
φ'	angle of internal friction	Slope of the failure line derived from the MC failure criterion
c'	Cohesion	failure line's y-intercept from the MC failure criterion
ψ	Dilatancy angle	Function of ε_a and ε_v
$E50$	Reference secant stiffness from drained triaxial test	y-intercept in $log(\sigma_3\|p_{ref}) - log(E_{50})$ space
ϑ	Poisson's ratio	0.3-0.4 (drained), 0.495 (undrained), 0.15-0.25 (unloading)
$K0nc$	Coefficient of earth pressure at rest (NC state)	$1-sin$ (default setting)

2.10.1 The Young's Modulus (E)

For uniaxial loading, Young's modulus is a key stiffness indicator that measures the relationship between soil stress and strain. The secant modulus at 50% strength, referred to as E50, is commonly used to represent the soil's response under loading conditions. In bi-linear stress-strain relationships, E50 remains constant, as illustrated in Figure 2-17.

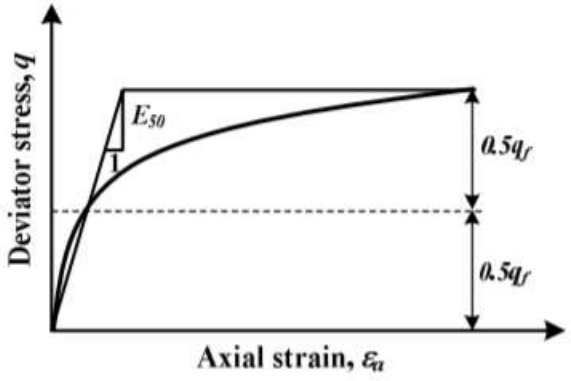

Figure 2-17 Definition of E_{50}

2.10.2 Poisson's Ratio (υ)

According to (Bowles 1988), the drained Poisson's coefficient of the soils under the loading scenario normally ranges from 0.3 to 0.4. The values for unloading scenarios range from 0.15 to 0.25. The Poisson's coefficient is 0.5 in a state that is not drained. However, using a precise undrained Poisson's ratio of 0.5 may make calculations more challenging. As a result, a value of u = 0.495 is proposed. According to Bishop and Hight (1977), accurately measuring Poisson's ratio requires precise strain measurements and calibration relationships. To preserve consistency with the PLAXIS formulation in the current example, the advice given in the PLAXIS Materials Model reference is followed.ulation challenges.

2.10.3 Cohesion (c')

The cohesiveness (c') factor includes a stressful dimension. The PLAXIS program advises using a low degree of cohesion (at least c' > 0.2 kN/m2) even in the case of cohesionless materials (c' = 0), in order to reduce computational issues.

2.10.4 Friction Angle (Φ')

Figure 2-15 (Mohr-Coulomb failure criterion) shows how to calculate the friction angle (Φ') using a plot of shear stress versus normal stress. The angle of friction is measured in degrees.

2.10.5 Dilatancy Angle (ψ)

It is indicated what the level of dilatancy is the dilatancy angle (ψ). Quartz sands typically have a dilatancy angle in the range of -30 degrees. However, cohesive clayey soils exhibit minimal dilatancy, except in heavily over-consolidated layers. In most cases, a dilatancy angle value of 0 would be suitable.

Table 2-4: Elastic constants of various soils(Samtani & Nowatzki, 2006)

Soil Type	**Poisson's Ratio, ν**
Clay: Soft sensitive Medium stiff to stiff Very stiff	0.3-0.5 (undrained)
Loess Silt	0.1-0.3 0.3-0.35
Fine Sand Loose Medium Dense Dense	0.25
Sand Loose Medium Dense Dense	0.20-0.36 0.30-0.40
Gravel Loose Medium Dense Dense	0.20-0.35 0.30-0.40
Es Calculation Using SPT N-value	
Soil Type	**Es (tsf)**
sand-filled silts, mildly cohesive mixes, and silts	$4N1_{60}$
Clean, fine to medium-sized sands with a minor siltiness	$7N1_{60}$
Sands that are coarse and have minimal gravel	$10N1_{60}$
Gravels and sandy gravel	$12N1_{60}$

3 RESEARCH METHODOLOGY

3.1 General

Urban regions frequently have deep excavations adjacent to existing structures, including buildings, substantial foundations, and underground pipelines. These buildings are vulnerable to changes in the earth brought on by excavation. Therefore, when designing and constructing deep excavations in such locations, it is crucial to consider and mitigate the potential adverse effects of excavation-induced ground movement, ensuring that they remain within acceptable limits. Instead of trying to prevent failure, the excavation design's main goal is to satisfy rigid displacement requirements. In these situations, the bottom-up construction strategy is frequently used. For our research, we specifically selected Kathmandu, a major city, due to the significant construction of tall structures in recent years. This choice allows us to study the challenges associated with deep excavations in densely developed urban areas and evaluate the effectiveness of different strategies for managing ground movements and minimizing their impact on surrounding infrastructure.

In this chapter field tests, as well as an explanation of the soil investigation's geology and geotechnical engineering characteristics, will be done at the Teku site. To conduct the parametric studies, an idealized excavation geometry is used. The chapter produces useful findings and conclusions that can be applied practically in the design and construction of deep excavations.

3.2 Introduction

Various methods have been used to carry out the numerical modeling of a cantilever pile wall. Chart presents a schematic summary of the various stages of the work.

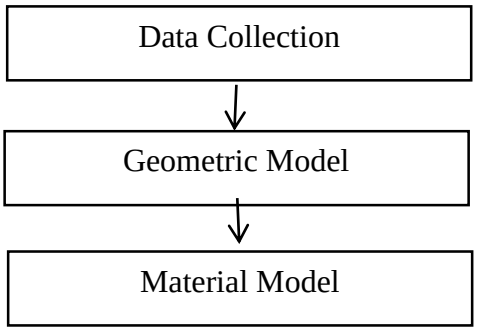

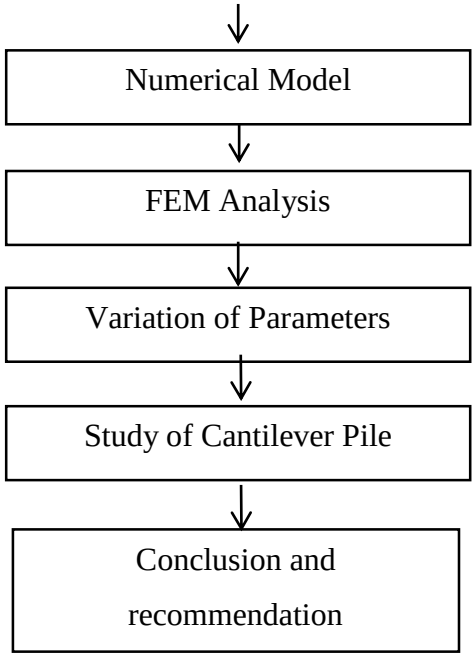

3.3 Data Collection

The Teku site's drilling testing provided the essential data for the parametric evaluation. The engineering and environmental geological map of the Kathmandu Valley was used to extract the soil parameters from the literature that was already available. The Kalimati Formation, a weakly consolidated sediment of Plio-Pleistocene age, contains the project site. The formation is predominantly made up of clayey silt and grey to black silty clay, with sporadic occurrences of phosphate minerals, calcareous sand, organic clay, fine sand beds, and peat layers. It should be noted that the project area is located in a region prone to hazards and foundation instabilities. Certain areas within the site have low bearing capacity, and settlement is a potential concern due to the presence of soft, silty clay, peat, and plastic soil below the soil cover. These factors contribute to the site's susceptibility to settlement issues.

The soil data comes from the proposed construction site of the National Public Health Laboratory in Teku, Kathmandu. Himalaya Geo Solution Pvt. Ltd. carried out the soil study in 2020 A.D., which included rotary drilling, Standard Penetration Test (SPT), and certain laboratory testing.

Field Investigation: Three boreholes were drilled to depths of 30m with Standard Penetration Tests (SPT) performed at 1.5m intervals. To conduct standard penetration test a split spoon sampler with an internal diameter of 35mm and an external diameter of 50mm was pushed by a 63.5 kilogram hammer that fell from a 760 mm height.

Water Table Monitoring: At least 24 hours after the borehole was drilled, the water level was measured. The water table was discovered at 3.6m depth in borehole one (BH-1), 4m depth in borehole two (BH-2) and borehole three (BH-3).

Natural Moisture Content and Bulk Density Test, Specific Gravity Test, Grain Size Analysis, Atterberg Limits Test, Consolidation Test and Unconfined Compression Test were all performed in the laboratory.

Bore Hole No.	Sample No	Depth m	Natural Moisture Content %	Grain Size Distribution %				Atterberg Limit, %			Unconfined Compressive Strength N/mm2	Consolidation Cc	Specific Gravity
				Gravel	Sand	Silt	Clay	LL	PL	PI			
BH - 1	DS	6	53.15		6.8	88.69	4.51	38.6	26.6	12			2.54
	DS	18	61.92		6.92	90.05	3.03	38.7	27.5	11.2			2.59
	DS	28.5	80.85		6.85	85.56	7.59	35.1	25.2	9.9			2.58
	UDS - 1	9.5	45.89		7.33	82.1	10.57				0.052		2.56
	UDS - 1	9.5	45.89		7.33	82.1	10.57					0.07	2.56
BH - 2	DS	4.5	34.61		7.53	85.01	7.46	38	27.6	10.4			2.57
	DS	7.5	31.6		6.61	82.74	10.65	34.9	24.3	10.6			2.44
	DS	15	48.61		6.37	89.05	4.58	35.6	27	8.7			2.59
	DS	21	51.02		7.52	89.47	3.01	32.4	21.7	10.7			2.6
	UDS - 2	12.5	65.06		6.61	82.74	10.65				0.054		2.56
	UDS - 2	12.5	65.06		6.61	82.74	10.65					0.07	2.56
BH - 3	DS	3	47.18		12.48	83.3	4.22	39.3	28.1	11.2			2.59
	DS	6	49.19		5.72	89.72	4.56	40.6	29.7	10.9			2.6
	DS	12	50.58		6.62	88.82	4.56	38.5	28.9	9.6			2.39
	DS	30	52.51		6.13	86.22	7.65	41.4	29.5	12			2.59
	UDS - 3	16	49.89		5.42	89.96	4.62				0.052		2.6
	UDS - 4	30	52.51		6.13	86.22	7.65				0.055		2.59
	UDS - 3	16	49.89		5.42	89.96	4.62					0.07	2.6
	UDS - 4	30	52.51		6.13	86.22	7.65					0.08	2.59

Figure 3-1 Summary of laboratory test results

The summary of the test results is given in above figure. Although the findings of the above-mentioned tests are nearly identical for all three boreholes, only the results of Borehole 2 (BH-2) are used in our analysis. The soil strata are medium soft to stiff blackish medium plastic clayey silt soil throughout the depth. Because the borehole is

only dug to a depth of 30m, the plaxis model assumes that this clayey layer extends to an unlimited depth.

The Mohr-Coulomb Model is utilized as the material model for the study of the model because the experiments required to get the data required for modeling soil using advanced material models such as hardening soil model and Modified Cam Clay model are not completed. We are unable to evaluate the applicability of a certain material model due to a lack of sufficient data, hence we are forced to adopt the Mohr-Coulomb material model in our investigation. Throughout the investigation, drained analysis is conducted.

3.4 Analysis of Data

The main tool for the analysis of data for this research has been considered is Finite Element Method with the use of 2D and 3D FEM software.

Both 3D and 2D finite element software were used for the examination of the cantilevered pile wall next to the excavation. We will go into more detail about the finite element model's dimensions, mesh characteristics, the choice of soil inputs, and the measurements and characteristics of the cantilever pile wall and the foundation of the building nearby in this part.

The steps involved in model formulation and calculation are:

- Defining a project
- Creating a soil profile using borehole data at the centre of model
- Material set creation to define the object
- Creating a volume using surface creation and extrude tools
- Material assignment
- Local refinement of mesh
- Mesh generation of model
- Defining calculation considering plastic calculation

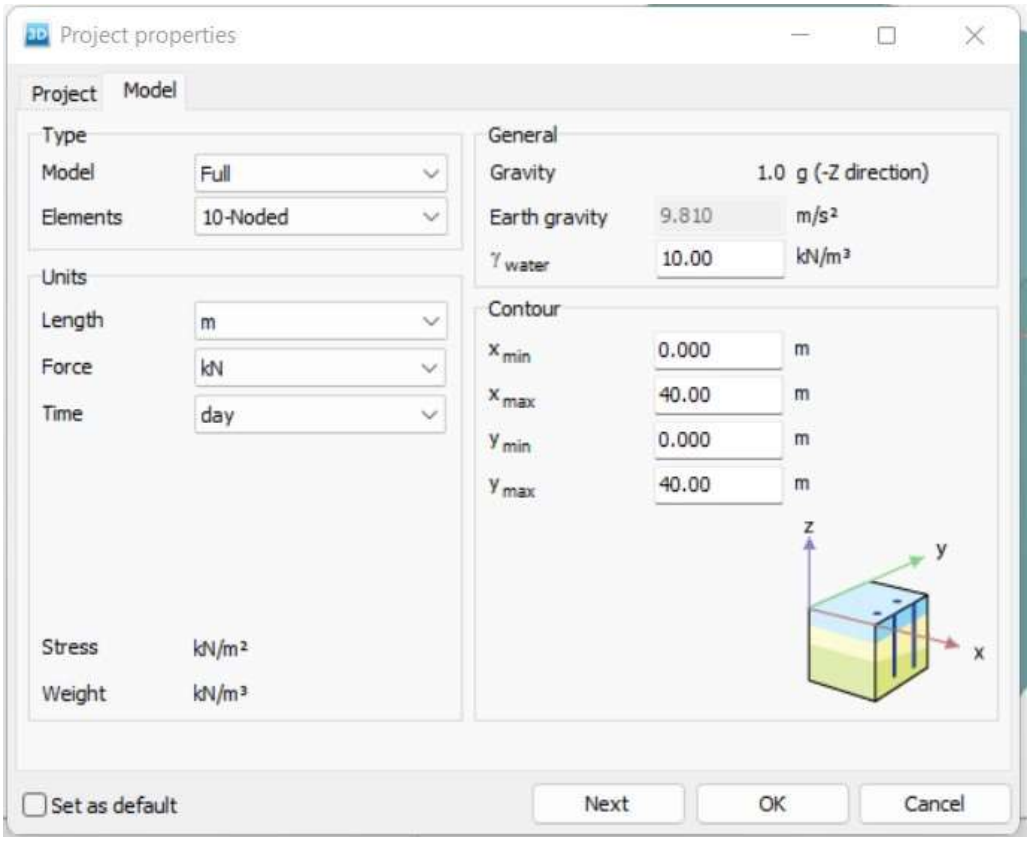

Figure 3-2: Input of Project Properties in PLAXIS 3D

3.4.1 Geometry and meshing

The bounds of the finite element model's size were determined with care to prevent any limitations or strain localization. The excavation area is 10 x 10 meters, and it is anticipated that the current building has the same proportions with a shallow footing 1.5 meters deep. Therefore the model's in-plane dimensions are set to be 30 x 20 m. It is important to note that three different types of footings for the adjacent building foundation are considered in the analysis. In the case of strip footings, it is anticipated that the soil will experience more pressures and deflections along the short than along the long side of the footing. In the case of soft clay, punching failure is anticipated, while for medium clay, local shear failure is expected, resulting in very small stresses and deformations that occur across the lateral direction. Because of the stress on the footing, as will be shown later, there is no localization of strain at the boundary conditions in the current analysis. Figure 3-3 depicts a cut perspective of the excavation, the surrounding soil, and the structure itself from the finite element model.

The only area supported by a cantilever pile wall is the excavation site next to the building's foundation; the other three sides are prevented from moving laterally in a perpendicular direction. In order to see the contour of the footing and the placement of the piles, the earth over the base level was removed. It should be noted, nevertheless, that the analysis still takes the removed soil into account.

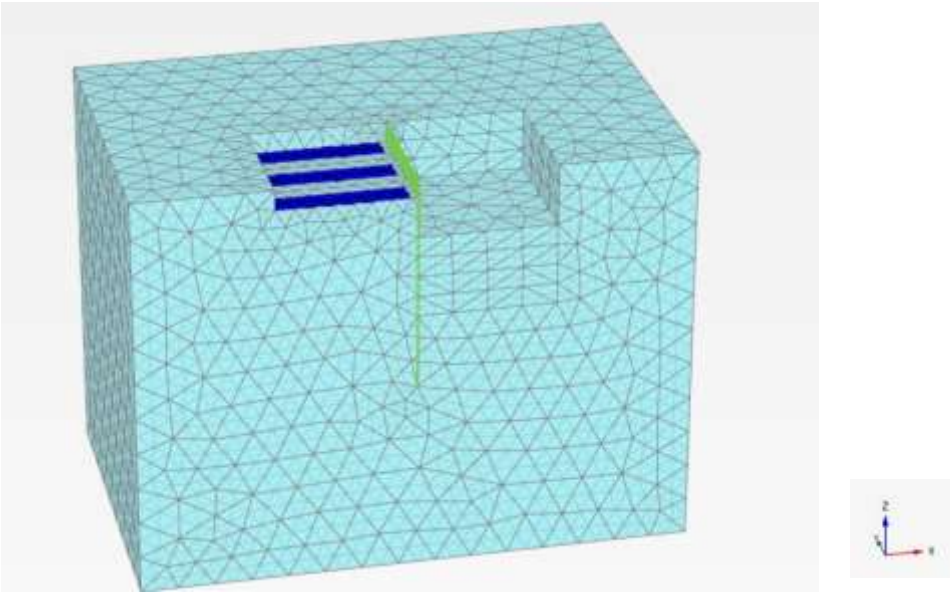

Figure 3-3: Mesh of finite elements for the excavation model -cut view

According to OU et al. (1996) the overall density of the mesh inside the excavation has a significant impact on the accuracy of the examination in three dimensions. The mesh was created as a fine mesh for the existing numerical model, as demonstrated in Figure 3-3.

3.4.2 Soil model

Secondary data for soil properties are utilized in the modeling process. Specifically, three distinct types of soil are considered for material modeling: cohesionless soil cohesive soil, and purely cohesive soil. These soil types are selected to accurately represent the characteristics of the actual soil in the analysis.

Firstly, Cohesive (C-φ) soil that is used in the model.

Table 3-1 Input Parameters Clay

Parameter	**Symbol**	**Soil** (0m-0.5m)	**Unit**
Material Model	Material Model	Mohr-Coulomb	
Saturated weight	γb	18.9	kN/m^3
Unsaturated weight	γb	17	kN/m^3
Modulus of Elasticity (Stiffness)	E	4800	kN/m^2
Stiffness Increment	E_{inc}	0	kN/m^2
Cohesion	C_u	27 &54	kN/m^2
Friction angle	φ(phi)	17	Degree
Poisson ratio	υ (nu)	0.3	-
Interface stiffness ratio	R_{inter}	1	-
Drainage Type	Drainage Type	Undrained	-

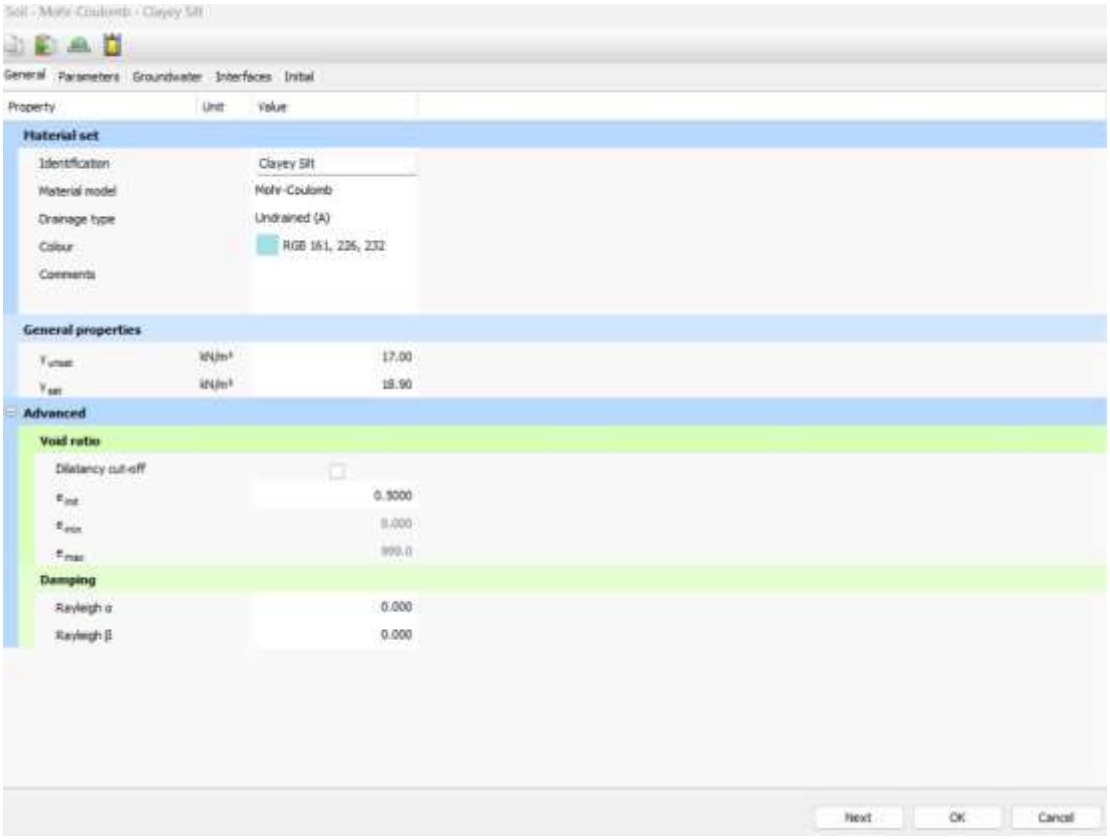

Figure 3-4 Input of soil Properties

3.4.3 An excavation support system

In this research, a cantilever pile wall was employed as a support structure for excavation. The pile wall was represented in the analysis as a solid, separate circular concrete pile that interacts with the surrounding soil at its outer interface. Different pile sizes and pile wall lengths that corresponded to various excavation levels were taken into consideration. The piles' center-to-center spacing was calculated to be twice the pile diameters. With a concrete modulus of elasticity of 2.5 x 10^7 kN/m^2, a Poisson's ratio of 0.2, and a unit weight of 25 kN/m^3, the pile material was considered to be linearly elastic. The pile's rough interface surface with the soil was also taken into consideration. Effect of grout element is also considered in this analysis. Grout element is modeled as plate element having thickness 0.3 m and material properties having same as that of concrete pile.

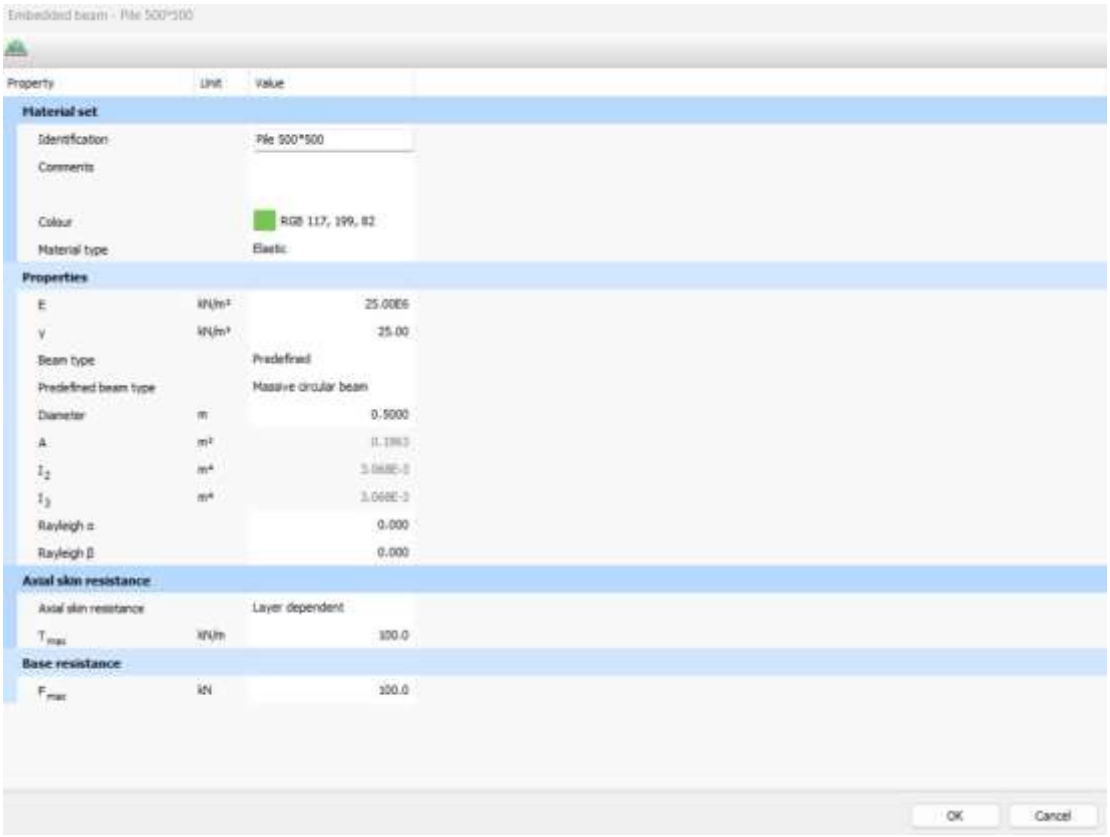

*Figure 3-5: Embedded beam (Cantilever Pile) 500*500*

3.4.4 Adjacent building foundation and its type

When analyzing the impact of nearby building loads on a pile wall supporting an excavation support system, the type of foundation is crucial. In analyzing the effect of adjacent building load on an excavation support system, three different foundation types are typically considered: isolated, strip, and mat foundations. Each type has unique characteristics and effects on how the pile wall and soil around it behave. In the analysis of the effect of adjacent building load on an excavation support system, it is necessary to consider the type of foundation present and its characteristics to evaluate potential soil movements, lateral pressures, and stability issues. Understanding the behavior of the pile wall and the surrounding soil is crucial for designing an appropriate excavation support system that can withstand the adjacent building loads while ensuring the safety and stability of the construction site. Footing base is considered at 1.5m depth beneath the ground level. The footing in the analysis was modeled as a linear elastic material having concrete properties, including a Poisson's coefficient of

0.2, a young's modulus of elasticity of 2.5 x 10^7 kN/m^2, and a unit weight of 24 kN/m^3. The pressures from a nearby structure were supposed to behave as an evenly distributed pressure on the foundation in order to make the modeling process simpler.

3.4.4.1 Isloated footing

An isolated foundation is a type of foundation that is typically used for individual columns or isolated structures. It consists of a concrete block that is isolated from the surrounding soil. Total nine numbers of square footing plate each of size 2*2 m were considered to model an adjacent building stress.

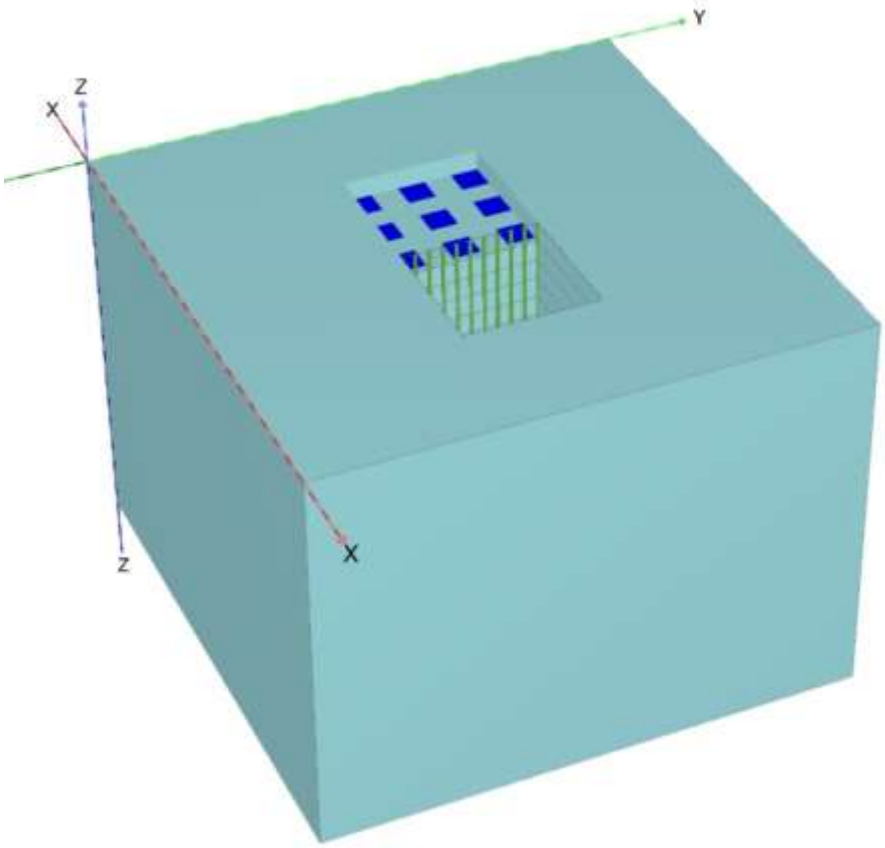

Figure 3-6 Isolated footing model

3.4.4.2 Strip footing

Three strip foundations were used to simulate the neighboring building's foundation in order to streamline the modeling process. The plates used to mimic these strip footings had dimensions of 0.5 m in thickness, 2 m in width, and 10 m in length. A rough

interface element that was automatically constructed was used to record the interaction between the footing elements and the earth.

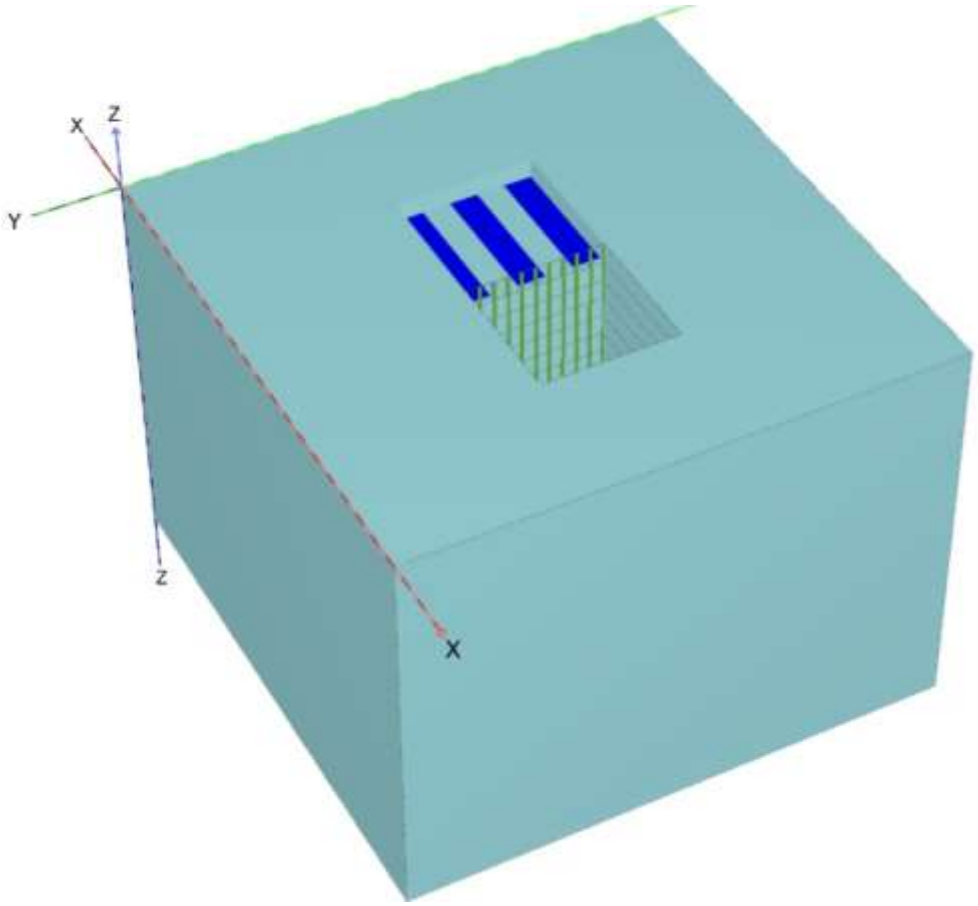

Figure 3-7 Strip footing model

3.4.4.3 Mat foundation

To study the effect of adjacent building foundation stress on excavation support system, the foundation is modeled as mat foundation. Plate element of 0.5 m thickness is considered.

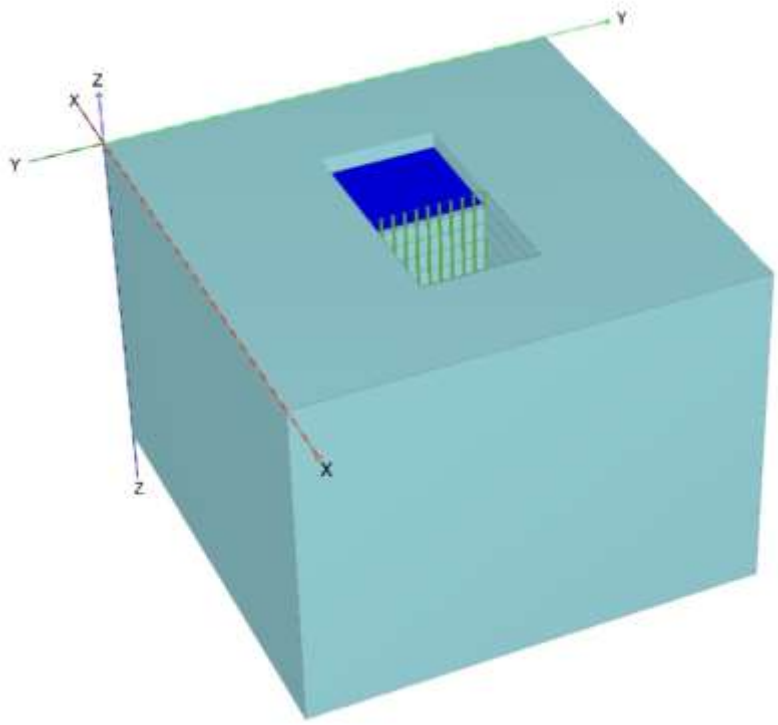

Figure 3-8 Mat foundation model

3.4.5 Stage construction

For the study, the analysis process was broken down into four parts. In the initial stage, the initial stress conditions were applied. The second stage involved activating the footings of the neighboring structure and applying pressure to them. In the third stage, the piles in the soil were activated. Finally, in the last stage, the soil excavation was performed to the desired depth.

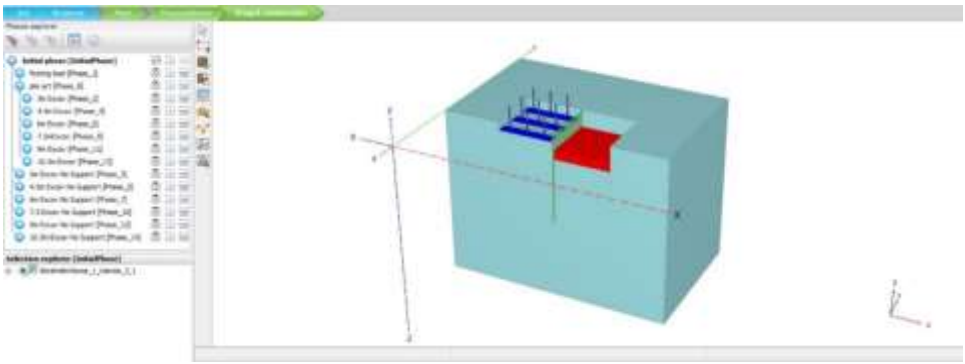

Figure 3-9: Stage Construction

4 RESULTS AND DISCUSSION

With the change of the design parameters, parametric analysis was conducted and adjacent building foundation types. The factors taken into account are length of the pile wall (Lp) = 18, 20, 22, 24, and 26m, embedment depth of pile (D), diameter of the pile (d) = 0.3, 0.4 & 0.5m, excavation levels from the ground surface (H)= 3, 4.5, 6, 7.5, 9 and 10.5m, soil's cohesion (c_u)= 27kN/m^2 and 54 kN/m^2 and load at neighboring structure base (q_s) = 100 and 200 kN/m^2.

4.1 Importance of Support System

The following figures demonstrate the distribution of soil displacement under vertical stress at nearby building foundation level100 kN/m^{2}at various excavation depths (H=3, 4.5, 6, 7.5, 9, and 10.5 m) with and without excavation supporting walls. There is less soil movement over the excavation line when a cantilever pile wall is employed to support it, especially below the basement level of the neighboring building. However, there is a modest reduction in the displacement of soil below the excavation level. This pattern is observed even when the soil has increased cohesion, resulting in smaller displacements due to the enhanced shear strength.

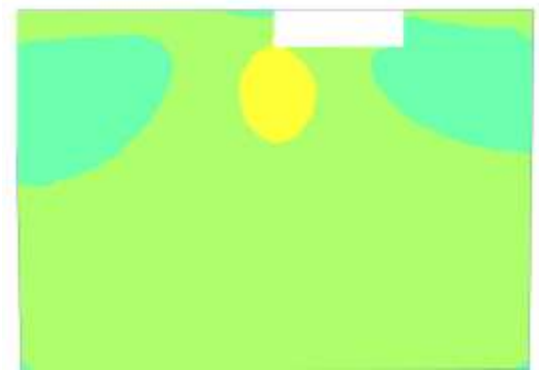

3m Excavation Without Support System

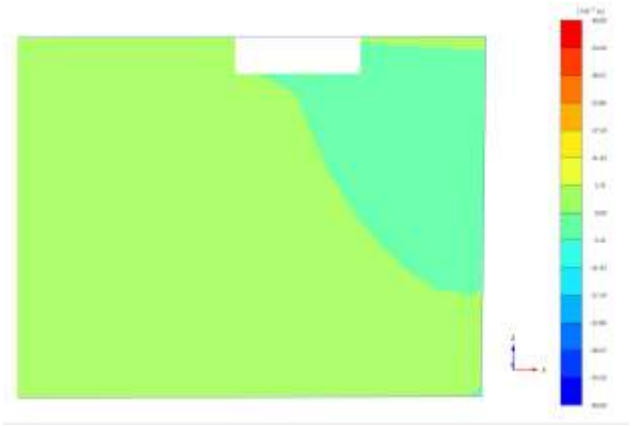

3m Excavation with Support System

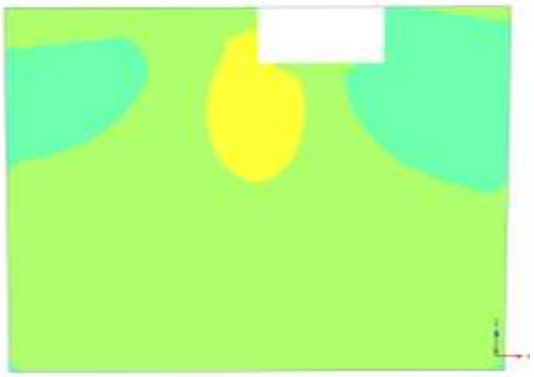

4.5m Excavation Without Support System

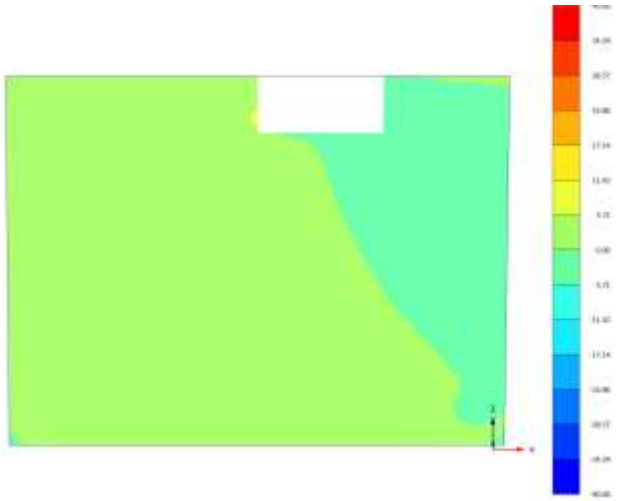

4.5m Excavation with Support System

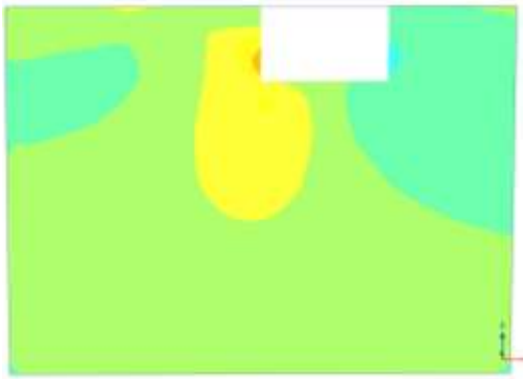

6m Excavation Without Support System

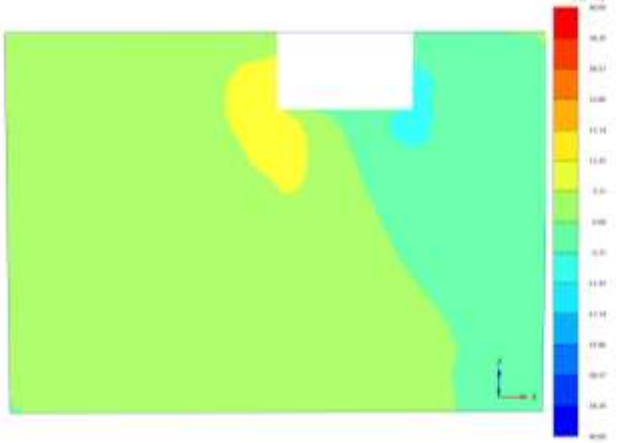

6m Excavation with Support System

7.5m Excavation Without Support System

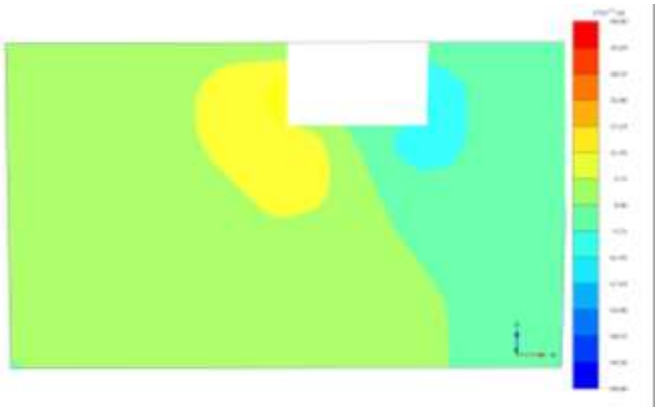

7.5m Excavation with Support System

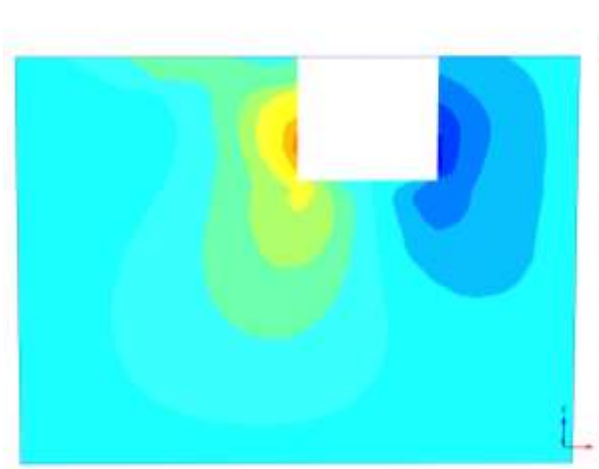

9m Excavation Without Support System

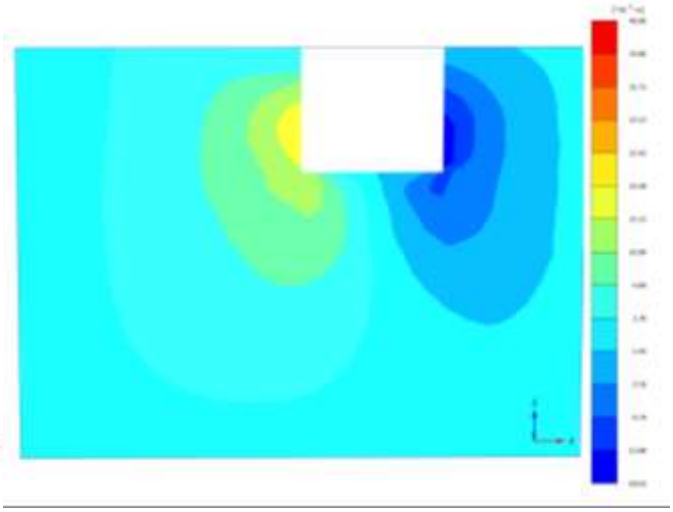

9m Excavation with Support System

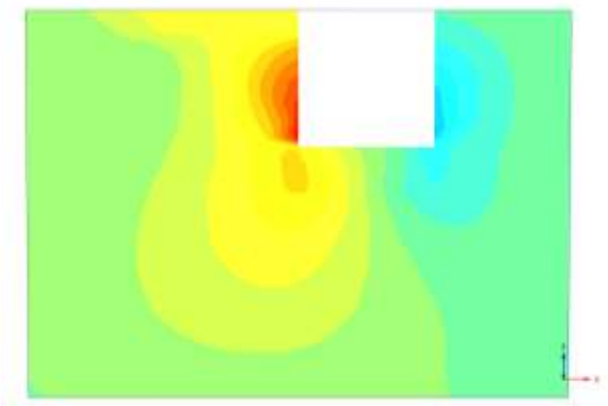

10.5m Excavation Without Support System

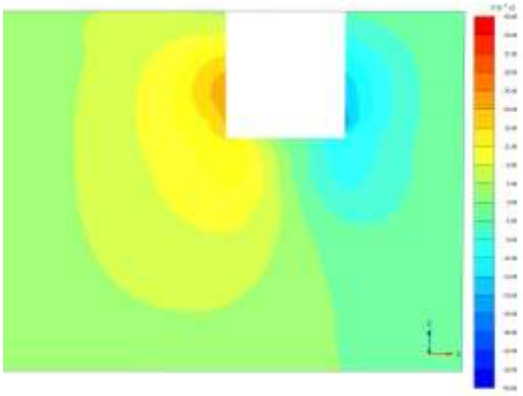

10.5m Excavation with Support System

Figure 4-1 Different excavation depths' lateral displacement distributions with and without pile wall support systems 3D

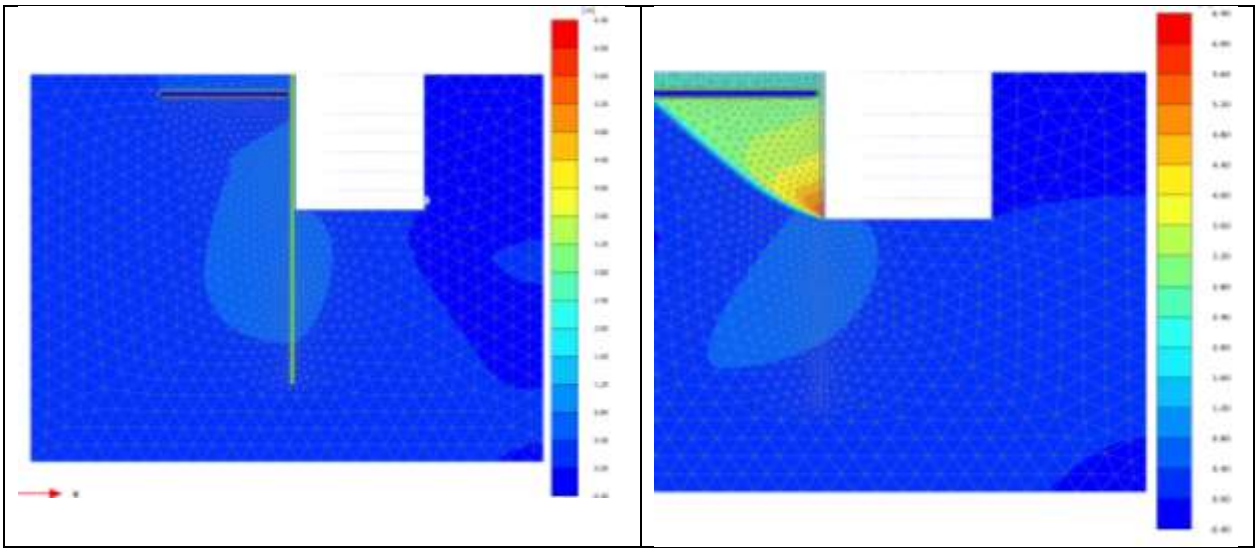

Figure 4-2 the distribution of lateral displacement for excavations of 10.5 meters deep with and without pile wall supports in 2D

4.2 Effect of Excavation Depth

The lateral deflection distribution for various excavation cases is illustrated in Figure 4-3. It can be seen that the lateral deflection values grow as the excavation depth rises for a certain embedded depth. This indicates that a greater excavation depth results in higher lateral pressure on the pile wall. The pile exhibits its maximum lateral deflection above the excavation level. However, for shallower excavations, near the excavation level is where there is greatest lateral displacement. As the excavation depth increases, the point of maximum lateral deflection gradually moves upward.

Figure 4-4 shows the bending moment distribution of pile for different excavation depths. The maximum bending moment occurs at the point of maximum lateral deflection. With increase in excavation depth bending moment also increases.

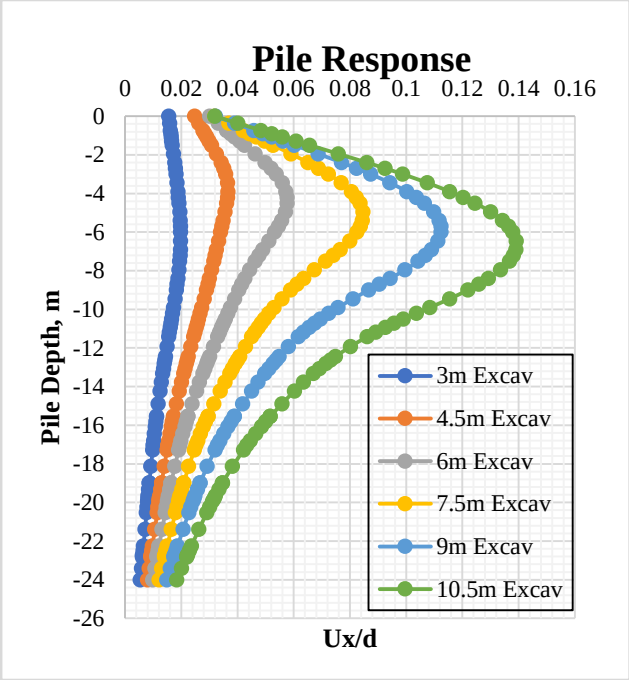

Figure 4-3 Lateral deflection for different excavation depths, pile length 24m, c_u = 27kN/m2 and q_s = 100 kN/m2

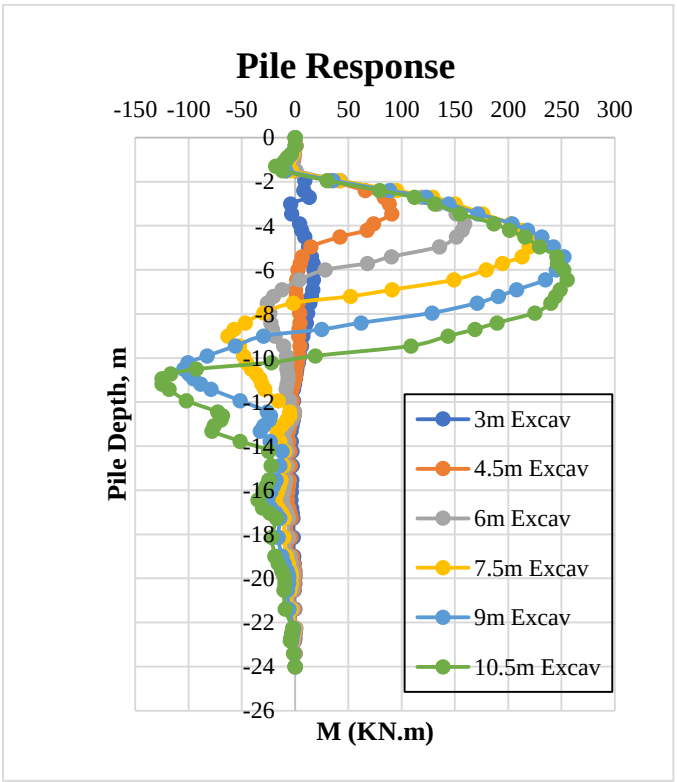

Figure 4-4 Bending moment for different excavation depths, pile length 24m, c_u = 27kN/m^2 and q_s = 100 kN/m^2

4.3 Effect of Clay Undrained Shear Strength

As demonstrated, the soil's undrained shear strength has a significant impact on lateral displacement of the soil. Figure 4-5 and Figure 4-6 shows distribution of pile wall lateral deflection for various cohesiveness values, c_u = 54, and 27 kN/m^2, at different pile wall lengths and for excavation depths 3, 4.5, 6, 7.5, 9 and 10.5m. Based on the observations made by Poulos and Chen (1995). It should be noted that there is a correlation between a decrease in lateral wall deflection and an increase in the soil's undrained shear strength (c_u). This suggests that when soil shear strength increases, soil movement decreases, resulting in less lateral wall deflection.

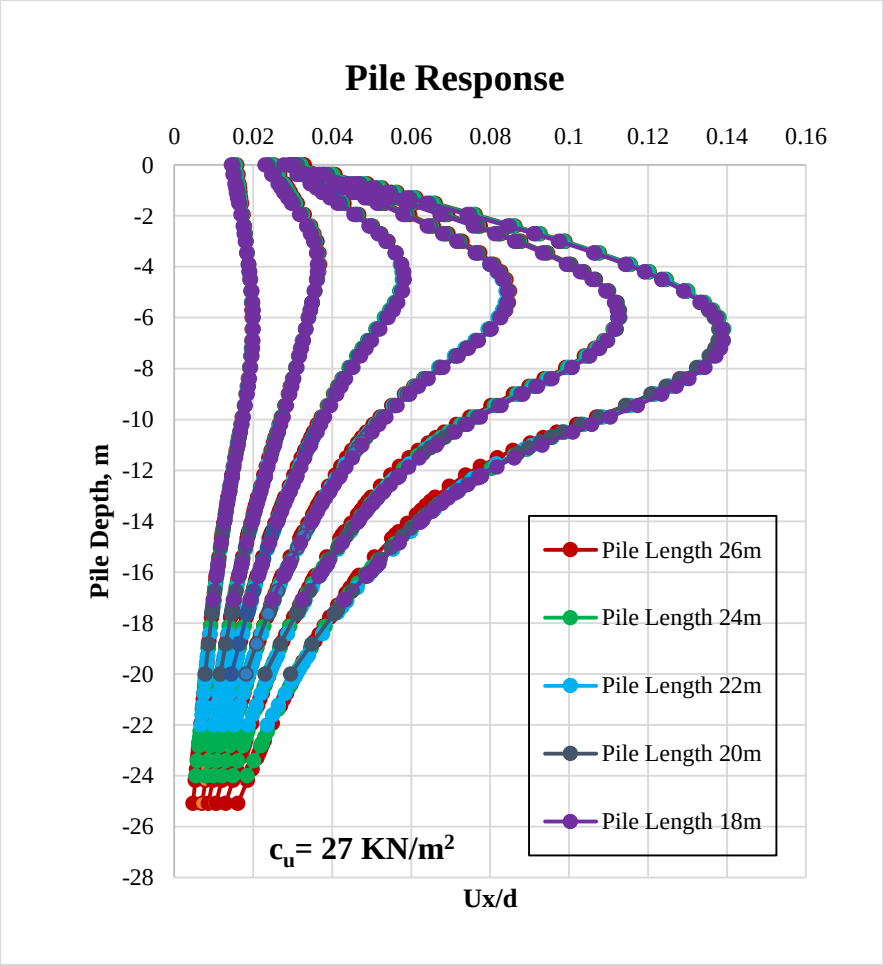

Figure 4-5 Distribution of lateral displacement in a pile wall for cohesiveness value, c_u= 27 kN/m^2 for different excavation depths

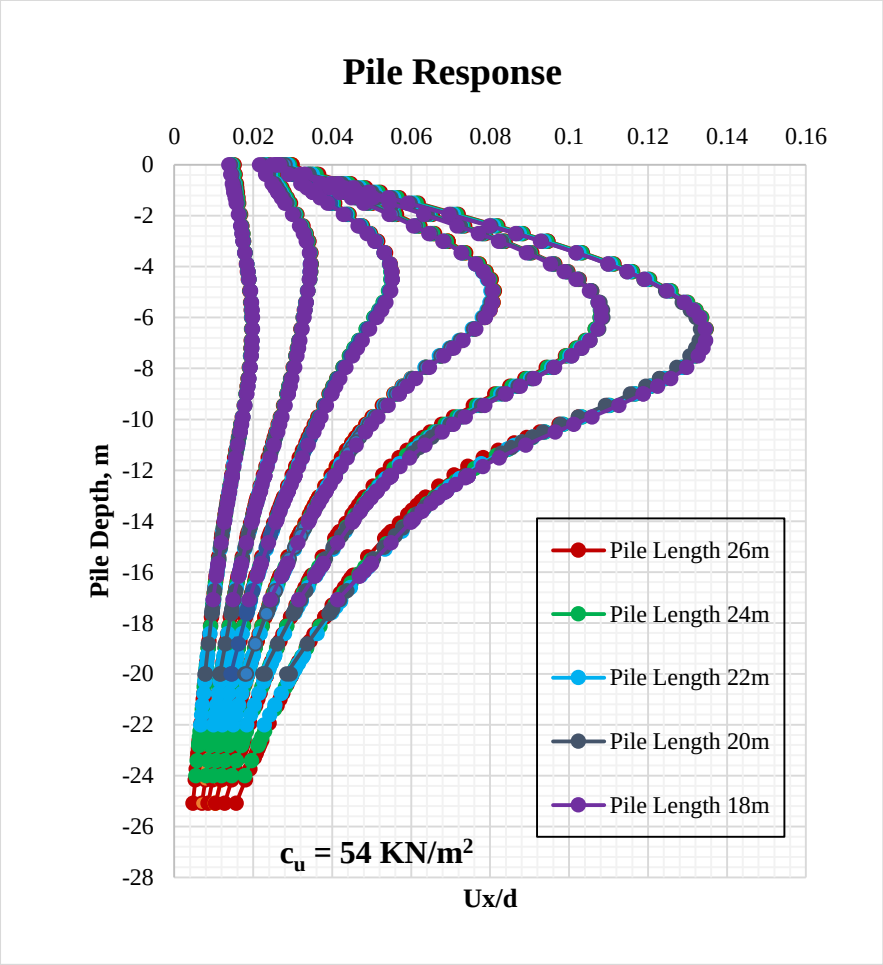

Figure 4-6 Distribution of lateral displacement in a pile wall for cohesiveness value, c_u= 54 kN/m^2 for different excavation depths

There is slight difference in bending moment with increase in undrained shear strength of soil. From the analysis it is shown that soil having lower value of internal friction angle exhibit larger change in lateral deflection and bending moment with increase in undrained shear strength of soil than that of higher friction angle.

Figure 4-7 and Figure 4-8 depicts the bending moment distribution of pile under adjacent building foundation load (q_s) 100 KN/m^2 , undrained shear strength (c_u) 27 KN/m^2 and 54 KN/m^2 for different excavation levels.

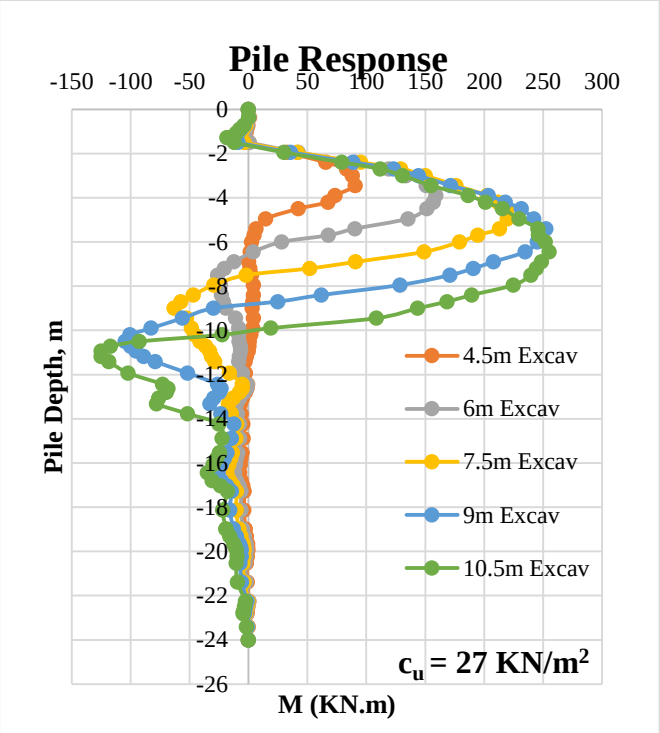

Figure 4-7 Bending moment for 24m pile length and excavation depth 3m c_u =27 kN/m² and q_s = 100 kN/m²

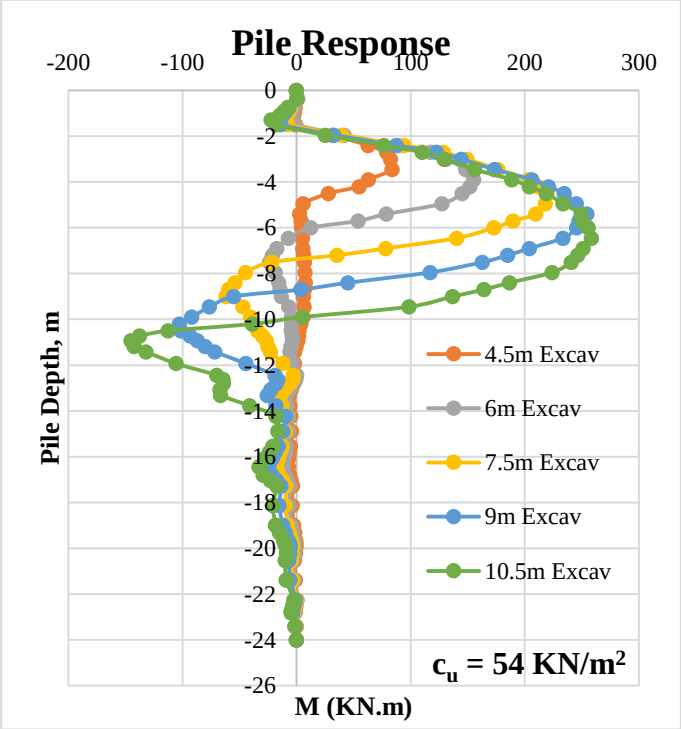

Figure 4-8 Bending moment for 24m pile length and excavation depth 3m c_u =27 kN/m² and q_s = 100 kN/m²

4.4 Effect of Applied Building Foundation Stresses (q_s)

The lateral displacement and bending within the pile wall are significantly influenced by the amount of applied load (q_s) at the neighboring building's foundation base. The distribution of lateral displacement in the piling wall for various values of q_s at the foundation level (-1.5 m) of the neighboring building is shown in Figure 4-9 for various wall lengths. The pile diameter is d = 500 mm and c_u = 27 kN/m^2. These statistics show that the amount of applied stress is a key factor in determining the size of the lateral displacement. Increasing the applied stress results in higher lateral deflection, indicating a direct proportionality between lateral deflection and the vertical stress at the foundation. The stiffness of the pile-soil system, the shear strength parameters (cu), induced soil pressure (that is determined by pressure), and the rigidity of the pile determine how much lateral movement increases. Thus, the lateral stress, lateral deformation, and bending moment felt within the pile are directly influenced by the applied stress.

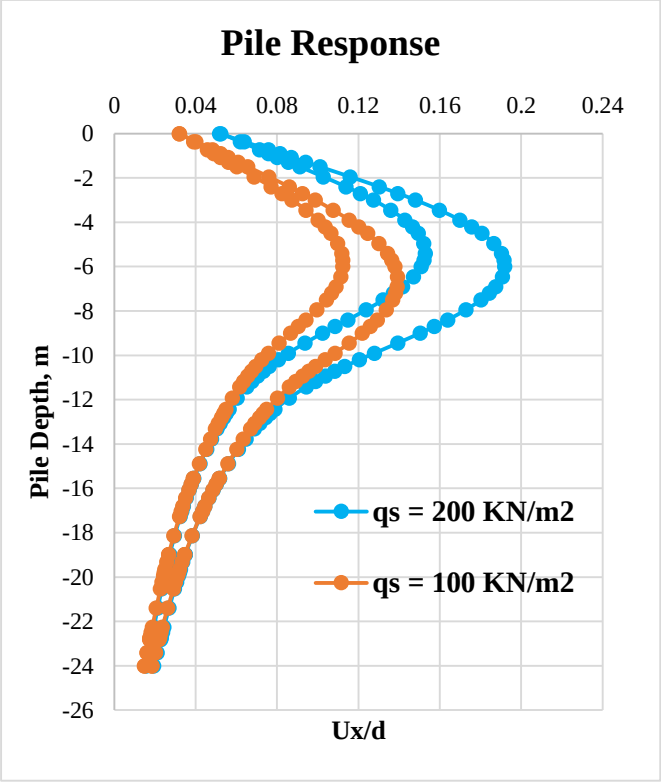

Figure 4-9 Distribution of Lateral displacement of pile wall for excavation depth 9 and 10.5m, q_s = 100 kN/m^2 and 200 kN/m^2 and c_u = 27 kN/m^2

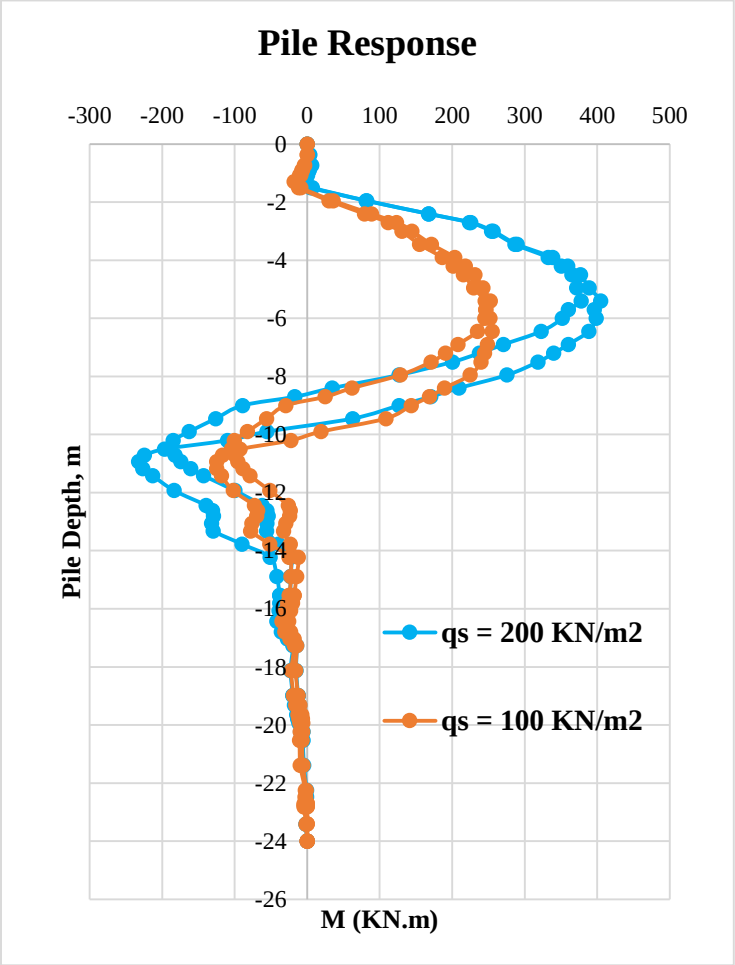

Figure 4-10 Bending moment distribution for excavation depth 9 m and 10.5 m, c_u =27 kN/m^2 and q_s = 100 & 200 kN/m^2

4.5 Effect of Pile Diameter

The lateral displacements were reduced while the bending moment was raised as the pile diameter (d) grew from 0.3 m to 0.4 m to 0.5 m. With increased pile diameter, the pile's bending moment on increases significantly. Figure 4-11 shows the lateral displacement and bending moment distribution of pile wall for different pile diameter (0.3m, 0.4m & 0.5m).

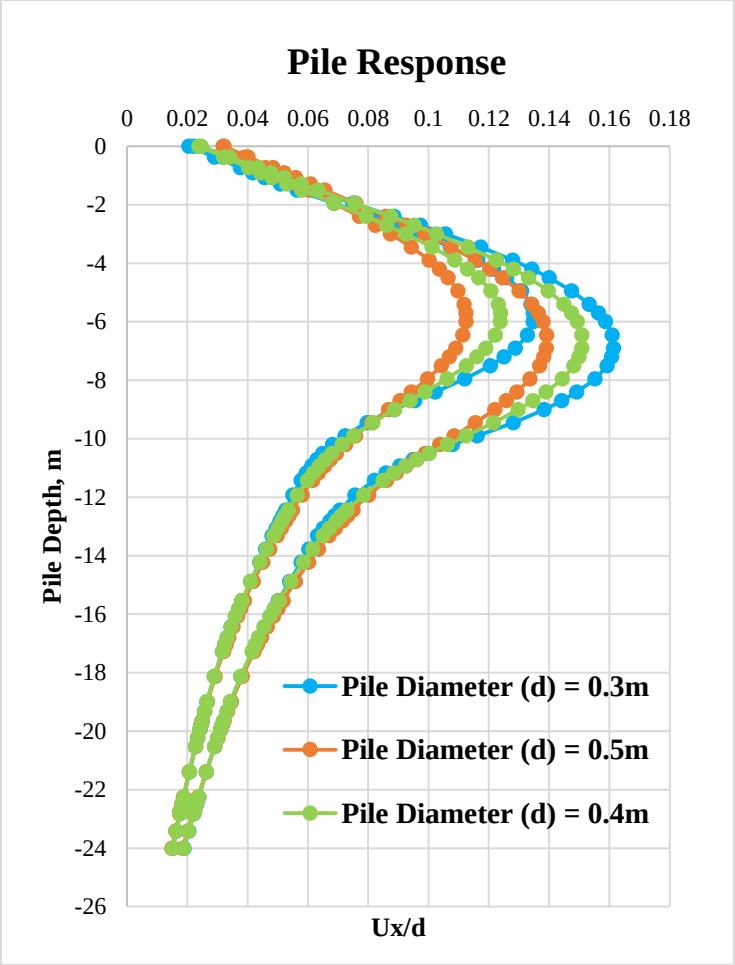

Figure 4-11 Pattern of lateral displacement of pile wall for excavation depth 9 and 10.5m, pile diameter (d) = 0.3, 0.4 & 0.5m, q_s = 100 kN/m^2 and c_u = 27 kN/m^2

For the same percentile increment of pile diameter, bending moment increasing magnitude is higher than in decreasing magnitude. For ±20% increment the maximum bending moment on the pile increases upto 63% and decrease 50% of that of base value. Figure 4-12 shows the bending moment distribution of pile wall for different pile diameter (0.3m, 0.4m & 0.5m).

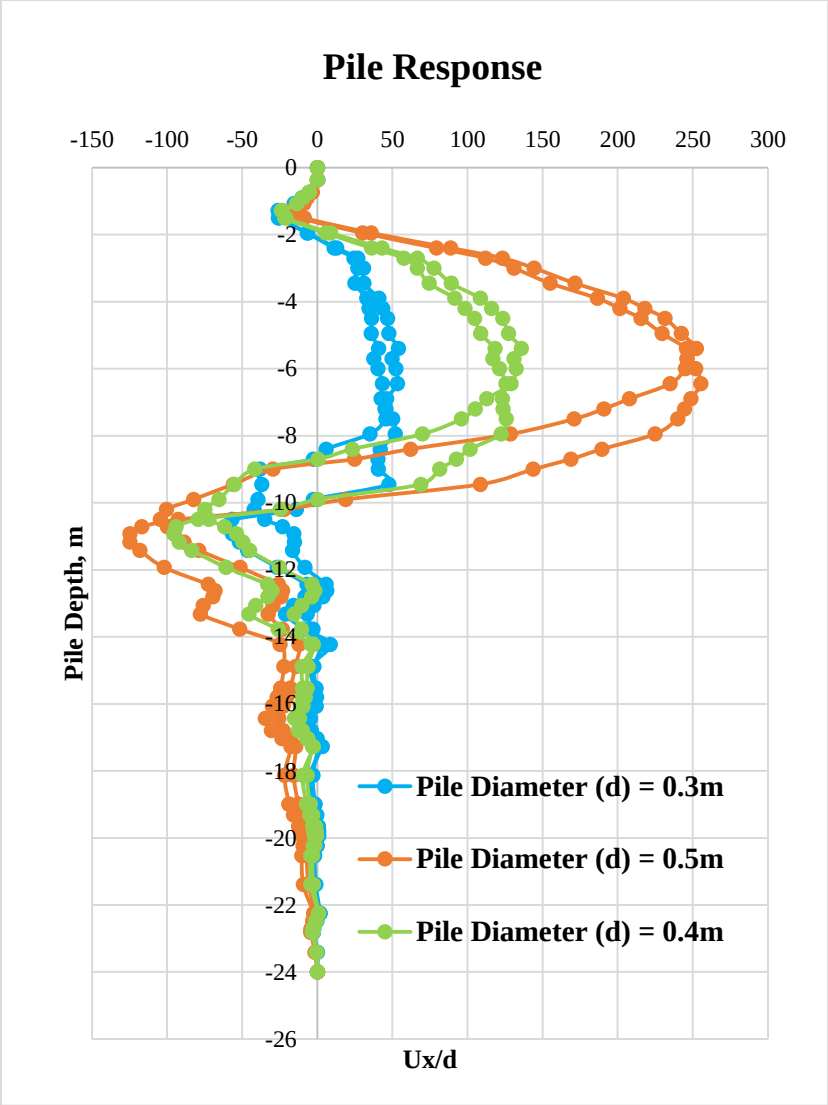

Figure 4-12 Pattern of bending moment of pile wall for excavation depth 9 and 10.5m, pile diameter (d) = 0.3, 0.4 & 0.5m, q_s = 100 kN/m^2 and c_u = 27 kN/m^2

4.6 Effect of Application of Grout Element

Application of 0.3m thick grout element on the excavation side reduces the lateral deflection distribution of pile wall significantly due to structural integrity of the pile wall and grout material. From Figure 4-13 it is shown that the maximum lateral deflection of pile wall with and without the application of grout element is 111mm and 140mm respectively. Application of grout element reduces the lateral deflection of pile wall by 20% of that of without grout application.

With the application of grout element increases the total rigidity and strength of the pile wall system. The added rigidity added due to grout element system also helps to limit the deformation of the pile wall during excavation. The grout element provides confinement to the surrounding soil, limiting its lateral movement. This confinement can reduce the soil's ability to deform and reduce the lateral pressure exerted on the pile wall, thus minimizing the risk of lateral displacement. By reducing lateral displacement, the grout element enhances the structural integrity of the pile wall system. It helps maintain the stability of the piles and prevents excessive bending or tilting, which could lead to structural failure.

Overall, the application of grout element on a pile wall to support excavation reduces lateral displacement by providing additional lateral support, transferring loads, increasing stiffness and strength, improving soil confinement, and enhancing the overall structural integrity of the system. This combination of factors helps to mitigate the risks associated with excavation-induced lateral movements.

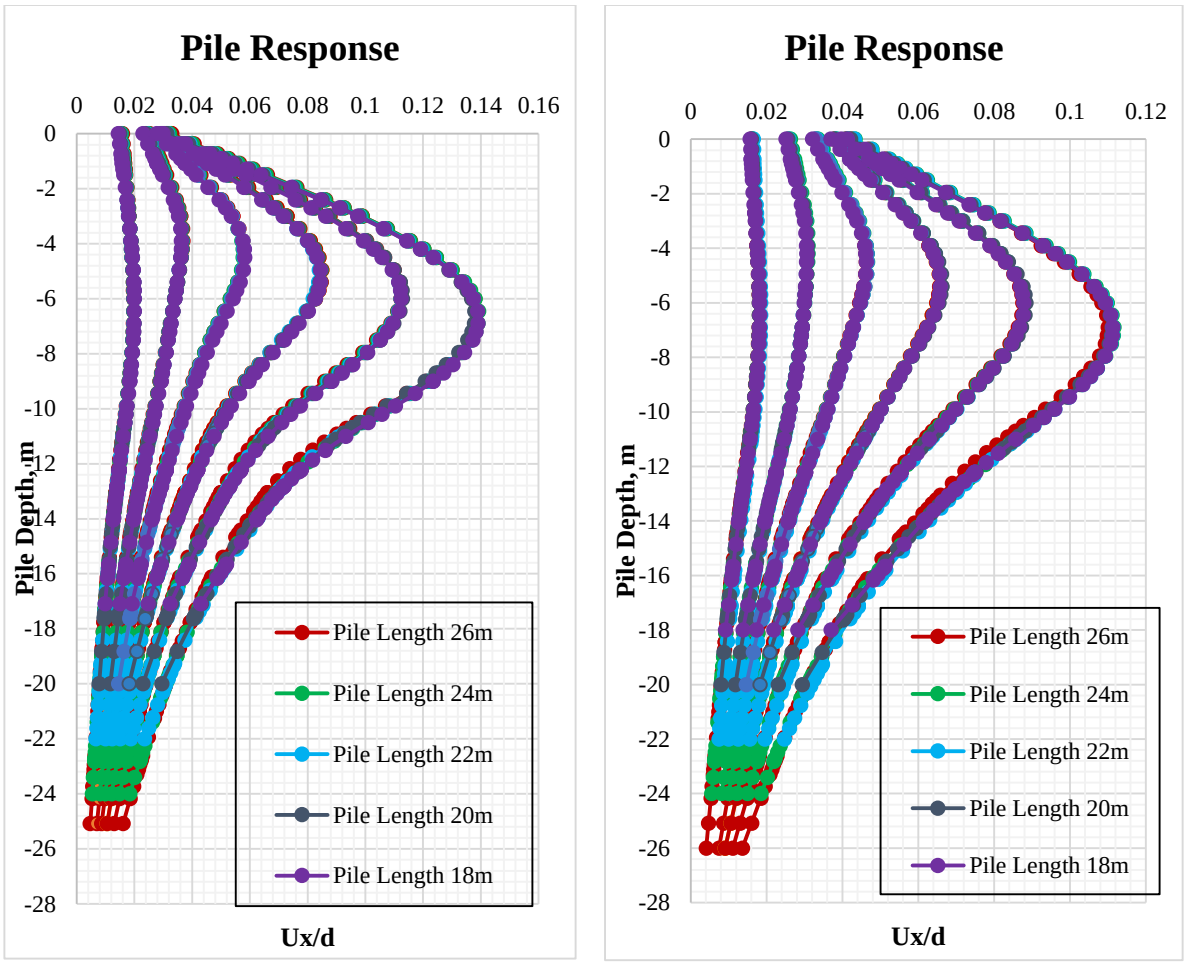

Without grout element

With grout element

Figure 4-13 Lateral deflection distribution of pile wall for different excavation depth, pile diameter (d) = 0.5m, q_s = 100 kN/m^2 and c_u = 27 kN/m^2 with and without the application of grout element

Also there is reduction in maximum bending moment of the pile wall with the application of grout element. Figure 4-15 shows the bending moment distribution of pile wall of length (l = 24m), diameter (d = 0.5m), soil undrained strength (c_u = 27 KN/m^2), & adjacent building foundation stress (q_s = 100 KN/m^2) with and without the application of grout element. It is clearly seen that grout element decreases the bending moment of pile wall as well as lateral deflection. The maximum bending moment reduces by 40% with the application of grout element.

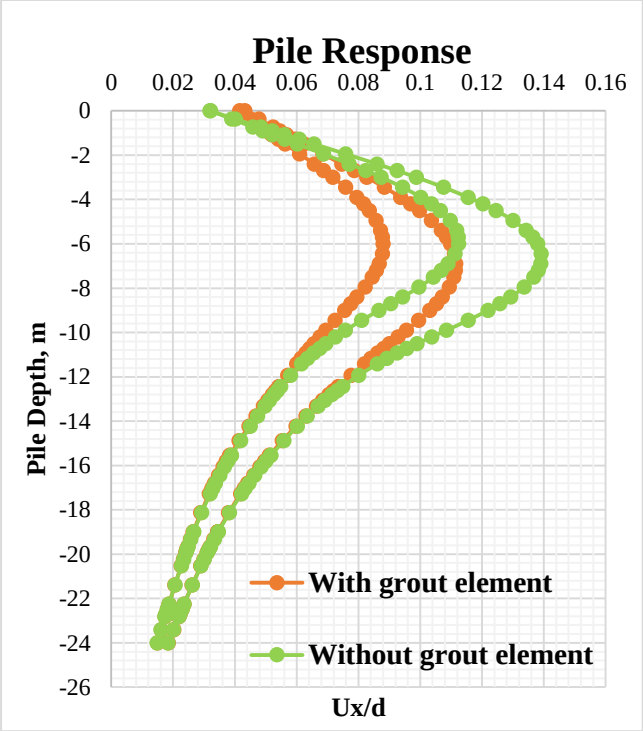

Figure 4-14 Lateral deflection distribution of pile wall for excavation depth 9 & 10.5m with and without the application of grout element

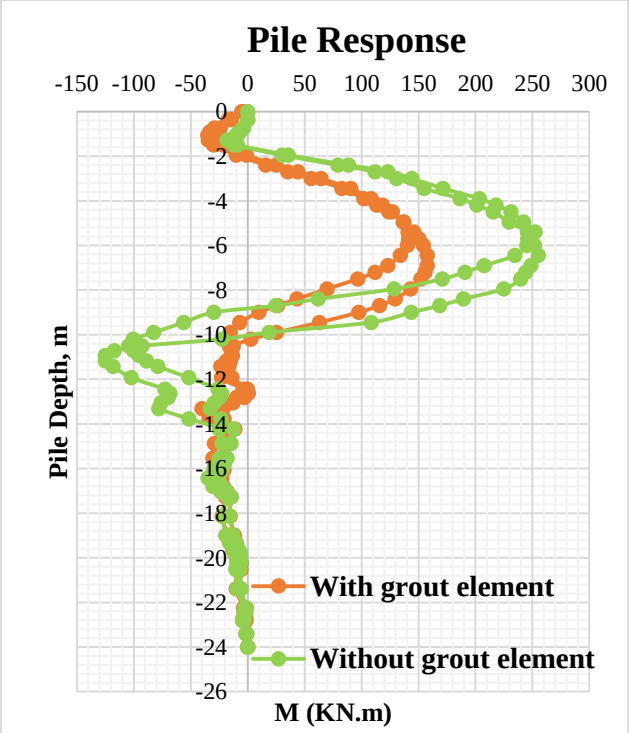

Figure 4-15 Bending moment distribution of pile wall for excavation depth 9 & 10.5m with and without the application of grout element

4.7 Effect of Adjacent Building Foundation Type

In this study for three different adjacent building foundation types, the deformation and bending moment performance of pile wall were analyzed with equivalent adjacent building load of (q_s) = 100KN/m^2, soil undrained shear strength of (c_u) = 27 KN/m^2 & pile diameter (d) = 0.5m. Mat foundation, strip footing and isolated footing were considered in this analysis.

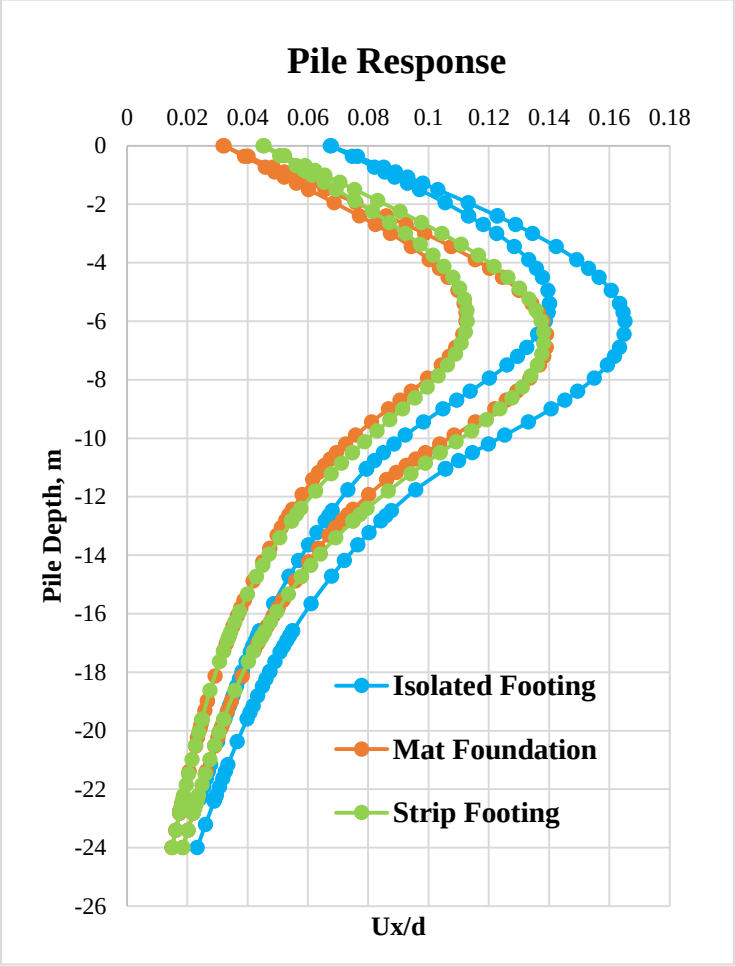

Figure 4-16 Lateral deflection distribution of pile wall for excavation depth 9 & 10.5m for three different adjacent footing types

From the analysis result it is shown that the lateral deflection of pile wall remains almost same in the case of strip footing and mat whereas bending moment increase in mat foundation case. For the isolated footing case the optimum lateral displacement of pile wall is higher than that of mat foundation and strip footing.

In the case of mat foundation and strip footing the maximum lateral deflection of pile wall were 139mm and 138mm respectively whereas isolated footing has maximum deflection is found to be 165mm which is almost 16% greater than that of mat and strip footing. In mat foundation and strip footing case

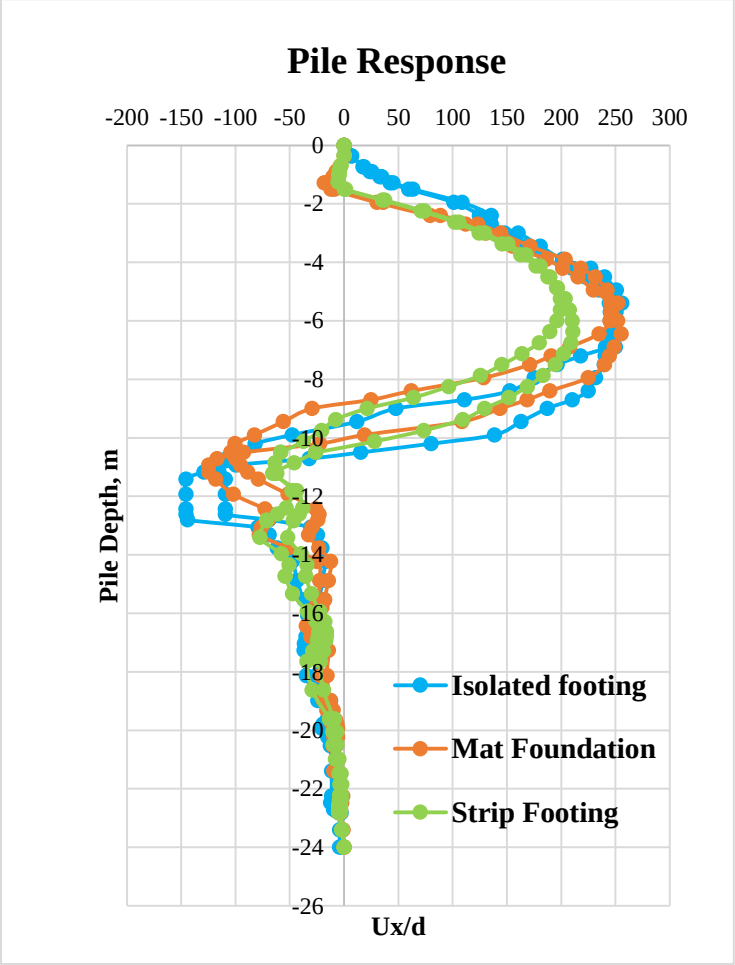

Figure 4-17 Bending moment distribution of pile wall for excavation depth 9 & 10.5m for three different adjacent footing types

The bending moment distribution on the pile wall for three different footing types are as shown in Figure 4-17. Isolated footing and mat foundation exhibit grater bending moment than that of strip footing.

4.8 Settlement of the Adjacent Building Foundation

The vertical settlement of adjacent building foundations near an excavation can be influenced by various factors, including the type of foundation used.

The building foundation was analyzed considering three different footings as mat, strip and isolated footing in 3D FEM analysis. With increase in excavation depth, the differential settlement of the foundation also increases. The settlement pattern of the adjacent building foundation is different for the excavation with or without support system as shown in Figure 4-18 and Figure 4-19. As the soil's cohesiveness value increases the settlement value decreases and increases with increase in applied foundation stress. As per IS 1904 the maximum permissible vertical settlement is 75mm for isolated footing case.

Maximum Vertical Settlement of the Adjacent Building Foundation (mm)						
Parameters	Without Grout Element			With Grout element		
	Isolated Footing	Strip Footing	Mat	Isolated Footing	Strip Footing	Mat
Pile diameter (d) = 0.5m	71.64	23.6	23.8	71.64	24.21	23.1
Undrained Shear strength (cu) =27 KN/m2	71.64	23.6	23.8	71.64	24.21	23.1
Adjacent Foundation stress (qs) = 100 KN/m2	71.64	23.6	23.8	71.64	24.21	23.1
Pile diameter (d) = 0.5m	72	23.8	24	70.1	24	23.4
Undrained Shear strength (cu) =27 KN/m2	77.7	22.8	22.4	70.68	21.3	22.6
Adjacent Foundation stress (qs) = 200 KN/m2	181	43.4	44.6	122.9	26.89	26.7

Generally speaking, isolated footings tend to experience more settlement compared to strip and mat foundations in such scenarios. This is primarily due to differences in load distribution and soil-structure interaction. Isolated footings are individual footing elements that support the load of a single column or pier. When an excavation is made near isolated footings, the soil around the excavation is disturbed, leading to a reduction in the lateral support provided to the footings. This reduced lateral support causes the footings to experience greater vertical settlement, as the load is less evenly distributed. The soil beneath the footings is more susceptible to consolidation, resulting in increased settlement.

On the other hand, strip and mat foundations are continuous footings that support multiple columns or walls. In the case of an excavation near strip or mat foundations, the presence of the continuous footing provides more lateral support to the soil surrounding the excavation. This distributed support helps to mitigate settlement and minimizes the differential movement of adjacent footings.

In summary, isolated footings are more vulnerable to settlement near excavations due to their individual nature and reduced lateral support, whereas strip and mat foundations offer better load distribution and lateral support, resulting in reduced settlement. However, it's important to note that site-specific factors, such as soil conditions, groundwater levels, and the depth and extent of the excavation, can also influence the degree of settlement for both types of foundations.

For small adjacent building load, the vertical settlement of the footing plate remains almost unchanged with and without application grout element whereas with increase in adjacent building load footing settlement with application of grout element is less than without grout element.

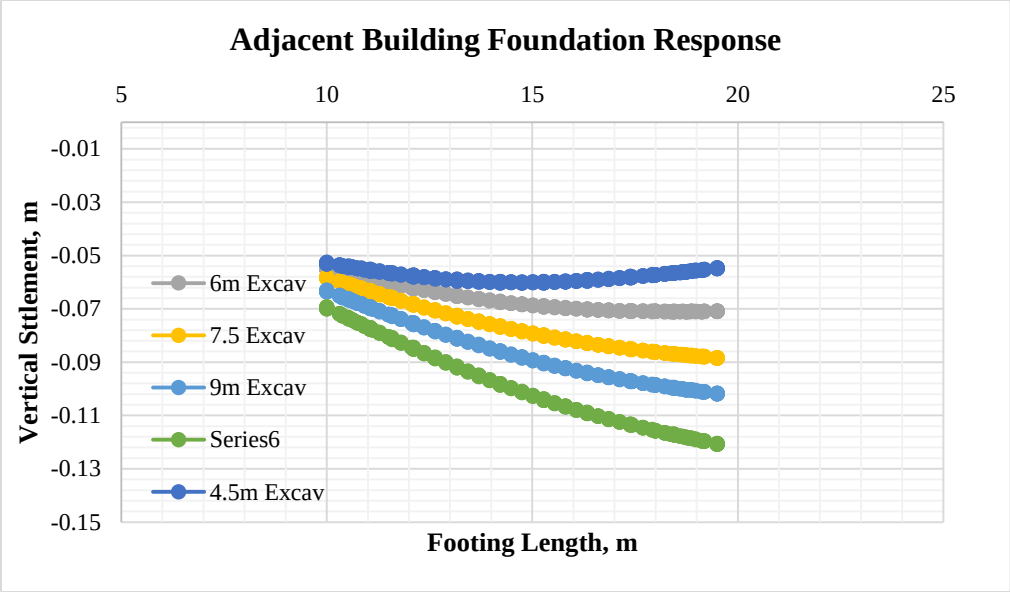

Figure 4-18 Vertical settlement of the building foundation for different excavation depths without pile wall support (pile length 24m)

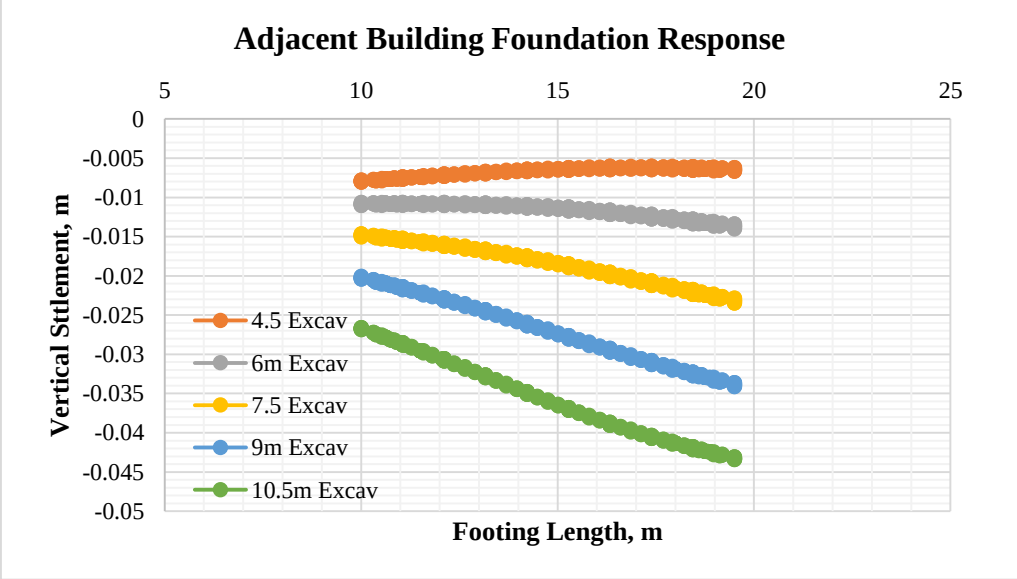

Figure 4-19 Vertical settlement of the building foundation for different excavation depths with pile wall support (pile length 24m)

With the application of pile wall as support system in excavation problem, the vertical settlement of the adjacent building can be reduced significantly as the application of pile wall reduces the excavation induced lateral soil movement.

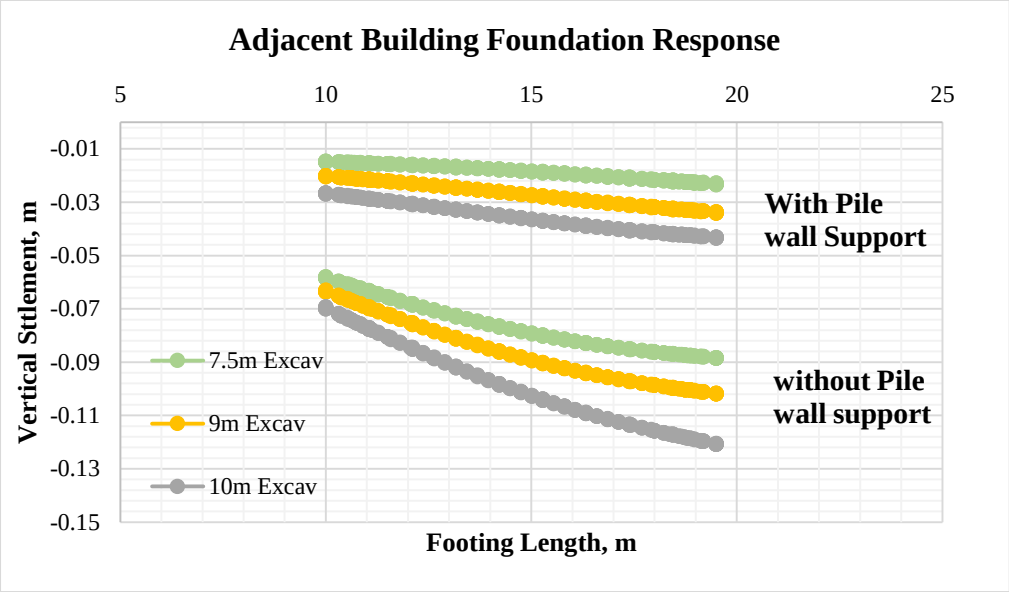

Figure 4-20 Vertical settlement of the building foundation for different excavation depths with and without pile wall support (pile length 24m)

4.9 Corner/edge effect

Lateral displacement distribution of pile wall is not same throughout the excavation side. From Figure 4-21 it is clear that at the corner side the lateral displacement decreases and is maximum at the center of the excavation face. In our study due to restriction of movement of soil in corner side there is reduction in the lateral displacement of pile upto length 2m from each corner and increase gradually to reach maximum value at center. Passive resistance developed at the corner side and its influence resist the movement of pile near corner. From figure it is shown that the center pile displacement is almost three times greater than that of edge pile displacement. So it is necessary to understand the edge effect in excavation support system design.

The corner piles are located in the corner of the excavation, where the unsupported soil area is relatively smaller compared to other sides. The smaller unsupported area results in reduced lateral movement of the soil and subsequently reduces the lateral deflection of the piles. In the corner side of the excavation, the presence of the adjacent soil on two sides provides additional lateral confinement to the piles. This confinement restricts the lateral movement of the piles and reduces their displacement. In the corner side, the pile wall interacts with two adjacent sides of the excavation wall, creating a

stronger and more stable structural system. This interaction enhances the overall stability of the corner piles and reduces their lateral displacement.

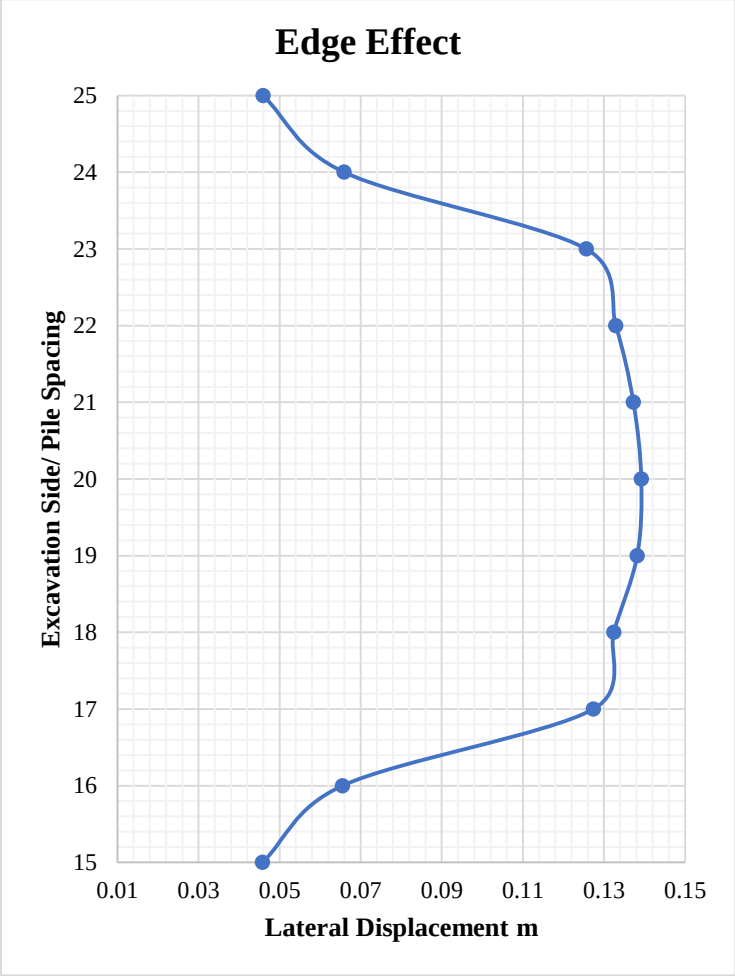

Figure 4-21 Corner effect in excavation side

4.10 Incremental variation of parameters

Taking consideration of soil undrained shear strength, friction angle and pile diameter the severity of these parameter with equal incremental is studied. Keeping base factors as soil undrained shear strength (c_u) = 27 KN/m^2, Friction angle 17^o and pile diameter = 0.5m, each parameter were varied -40 % to +40% and result were studied. From Figure 4-22 it can be concluded that with decrease in cohesion, friction angle and pile diameter increases the lateral displacement of pile among them reduction in cohesion

results greater displacement increase. Increase in above parameter, increase in pile diameter results minimum lateral displacement than other two factors.

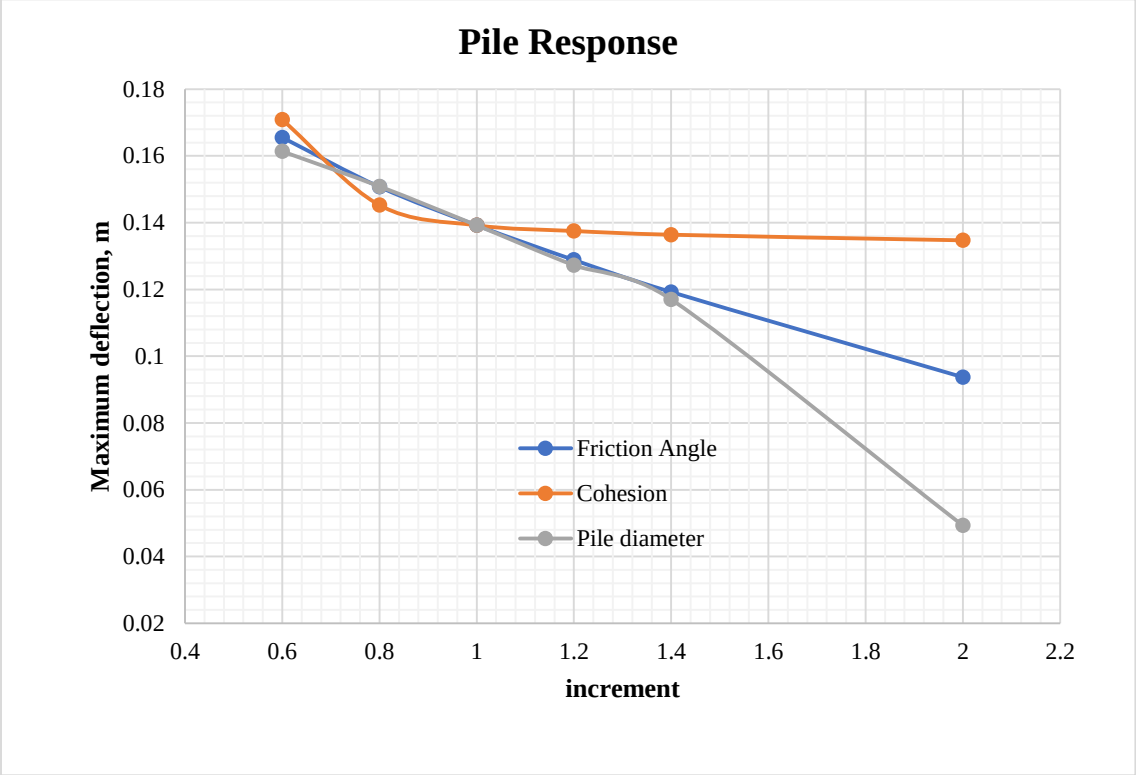

Figure 4-22 Incremental variation of parameters

In soils with a higher frictional angle (i.e. 17° in our study), the resistance to shearing is predominantly governed by the frictional forces between soil particles. As the cohesive vlaue of the soil increases, it enhances the overall shear strength of the soil, including the resistance to lateral movement. Therefore, an increase in cohesion has a minimal impact on the lateral deflection of a pile in such soils since the soil's strength is already dominated by friction.

However, in soils with a lower frictional angle the cohesion of the soil becomes a more significant factor in controlling its shear strength. When the cohesion of the soil increases, it directly increases the soil's shear strength, which in turn leads to a reduction in lateral deflection of a pile. In this case, the increase in cohesion has a more pronounced effect on the soil's behavior, resulting in decreased pile deflection.

4.11 Comparison of 2D FEM Analysis Result with 3D FEM Result

Plaxis 2D and Plaxis 3D software were used to compare the results of 2D and 3D modeling of the excavation support adjacent to old building.

The calculation results obtained with Plaxis 2D software are shown below.

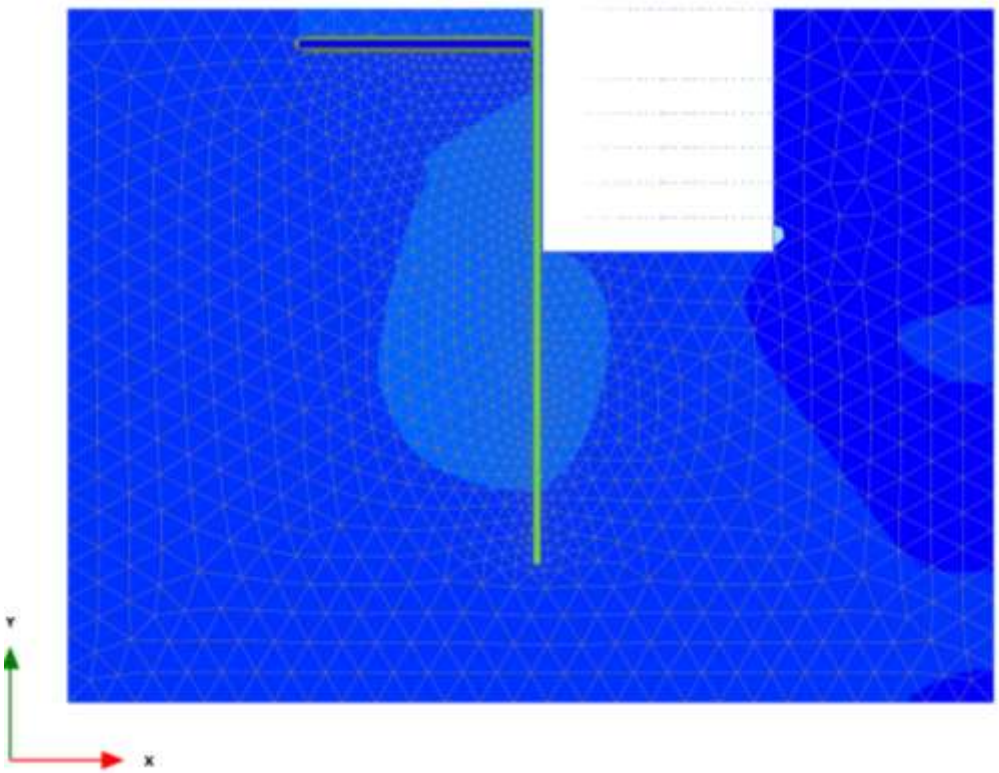

Figure 4-23 Plaxis 2D model (excavation depth of 10.5,0 m)

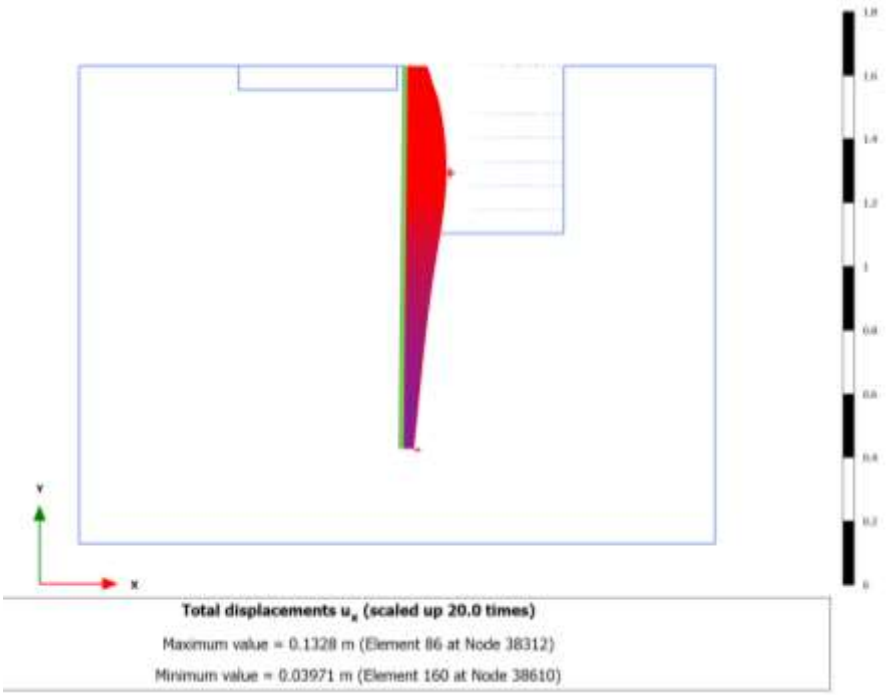

Figure 4-24 Displacement of pile wall (Plaxis 2D)

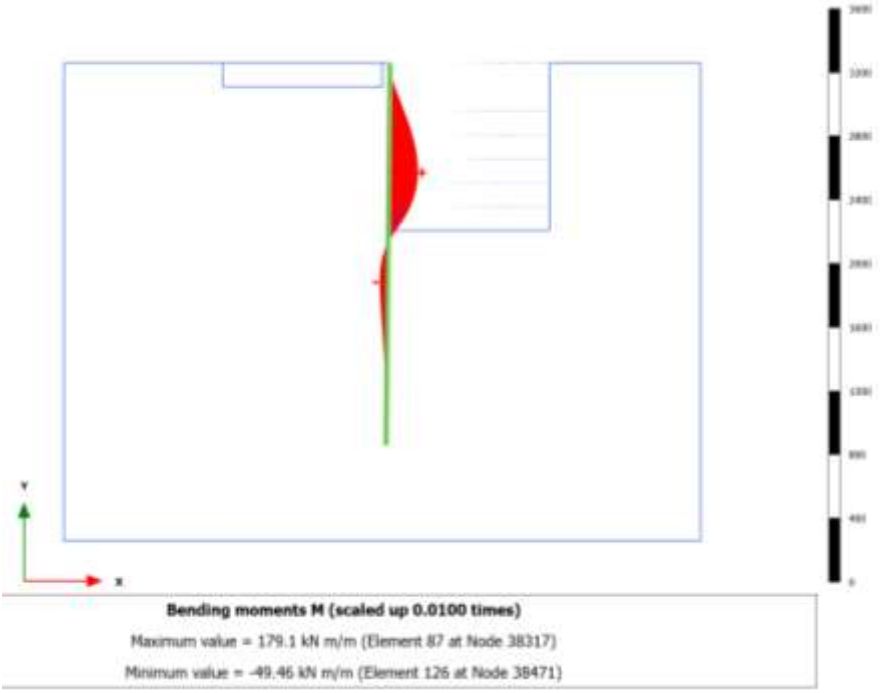

Figure 4-25 Bending Moment of the Pile wall supporting excavation (plaxis 2D)

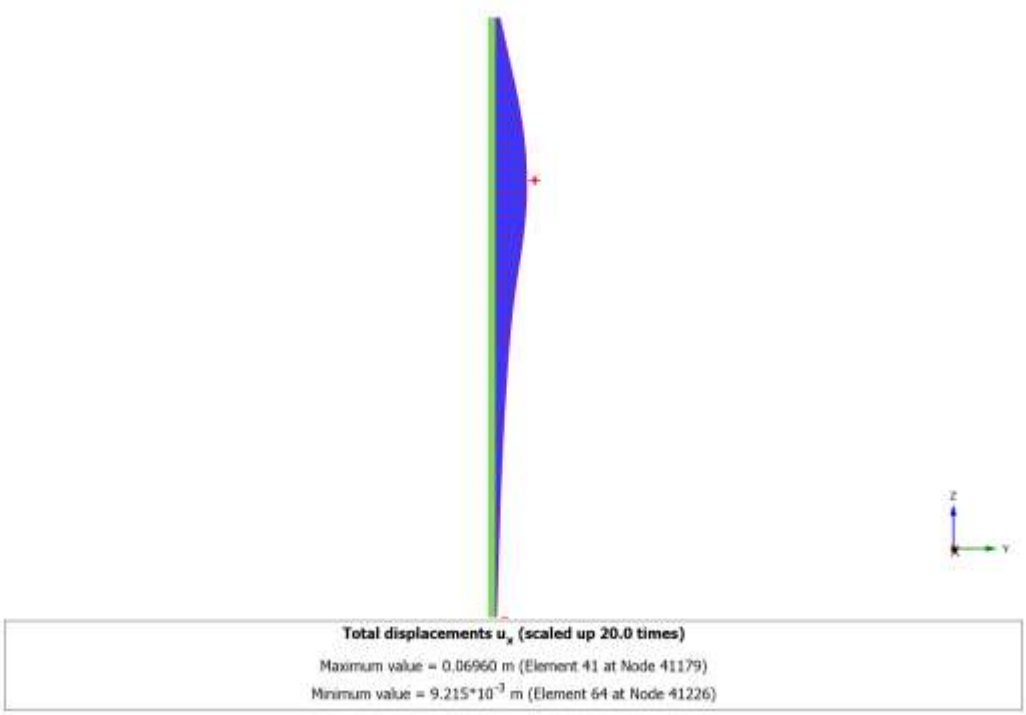

Figure 4-26 Maximum displacement of pile wall supporting excavation (plaxis 3D 10.5m depth)

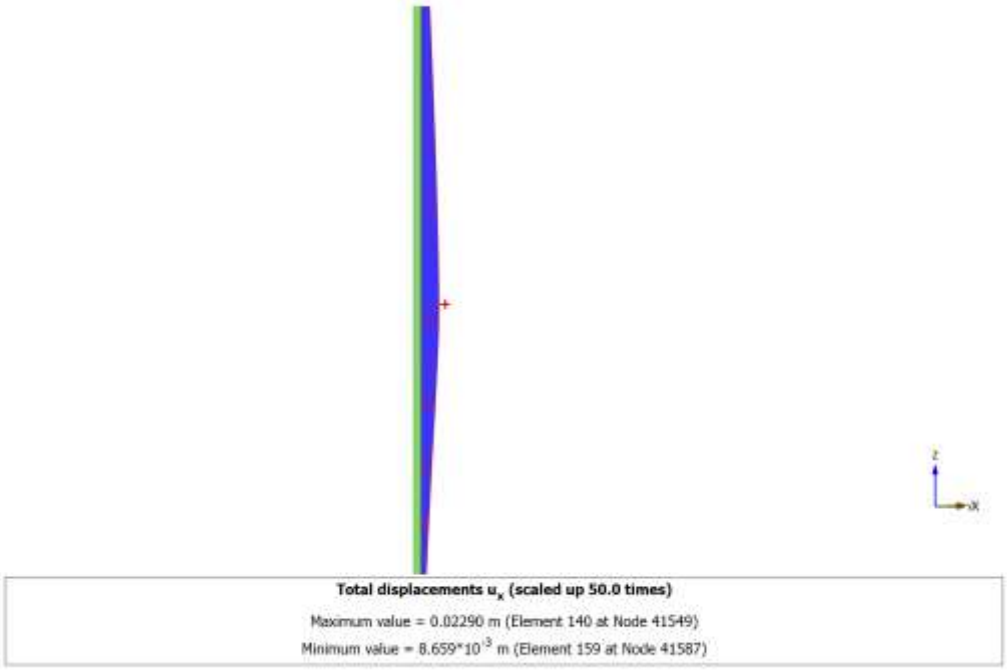

Figure 4-27 Minimum displacement of pile wall supporting excavation (plaxis 3D 10.5m depth)

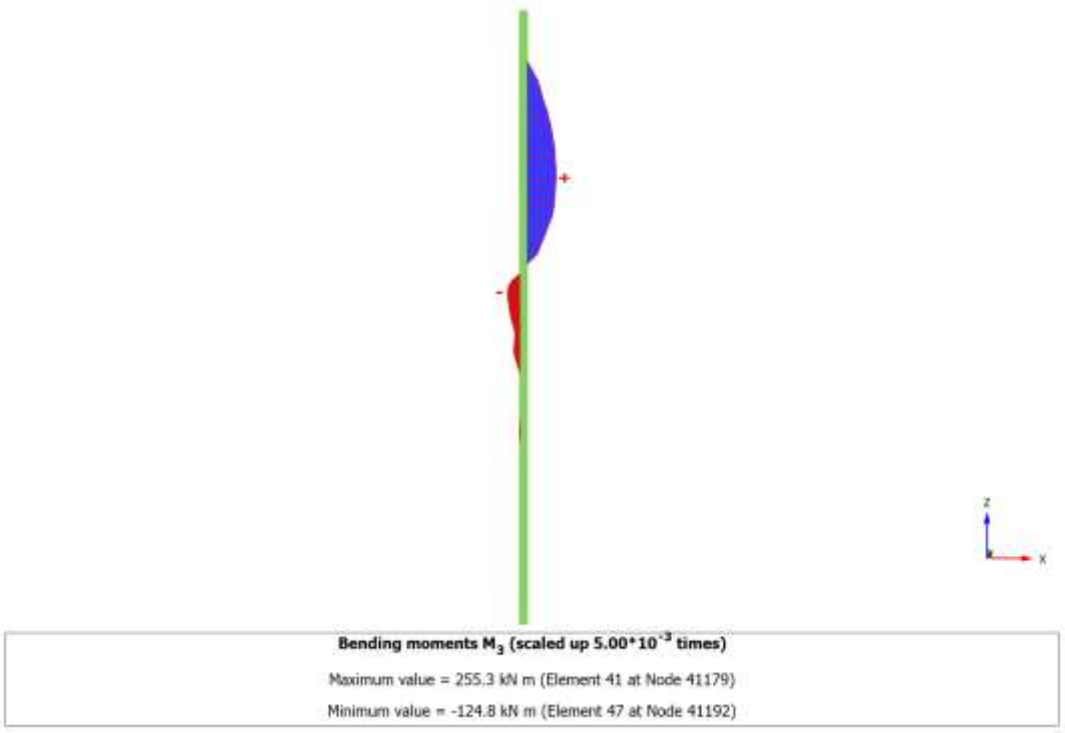

Figure 4-28 Bending moment distribution of pile wall (plaxis 3D)

From above figures It is evident that the pile wall's maximum predicted horizontal deflection by plaxis 2D is 0.132m which is higher value than 0.069 obtained by plaxis 3D. Also for the piles near corner of the excavation plaxis 2D calculates same results where plaxis 3D calculates different for each individual pile. The minimum lateral deflection by plaxis 3D is 0.0229m. plaxis 2d computed corner pile lateral displacement is almost six times greater than that of plaxis 3D. Similarly the maximum bending moment calculated by 2D FEM is less than 3D FEM analysis.

Plaxis 2D calculates the maximum estimated bending moment of the pile wall to be 179.1 kNm, which is significantly greater than the 255.3 kNm computed by Plaxis 3D. The maximum bending moment produced by Plaxis 2D analysis is 30 % less than by Plaxis 3D. Plaxis 2D's maximum computed horizontal displacement of the pile wall is 92% greater than Plaxis 3D's. Following figure show the lateral deflection distribution of pile wall in plaxis 2D and 3D. That is due to the 2D analysis's plain strain modeling. It is expected in plain strain models that there will be uniform loading, uniform ground

conditions, and zero displacements on the side that faces the model. Additionally, the discontinuities are disregarded and the structure is believed to be uniform.

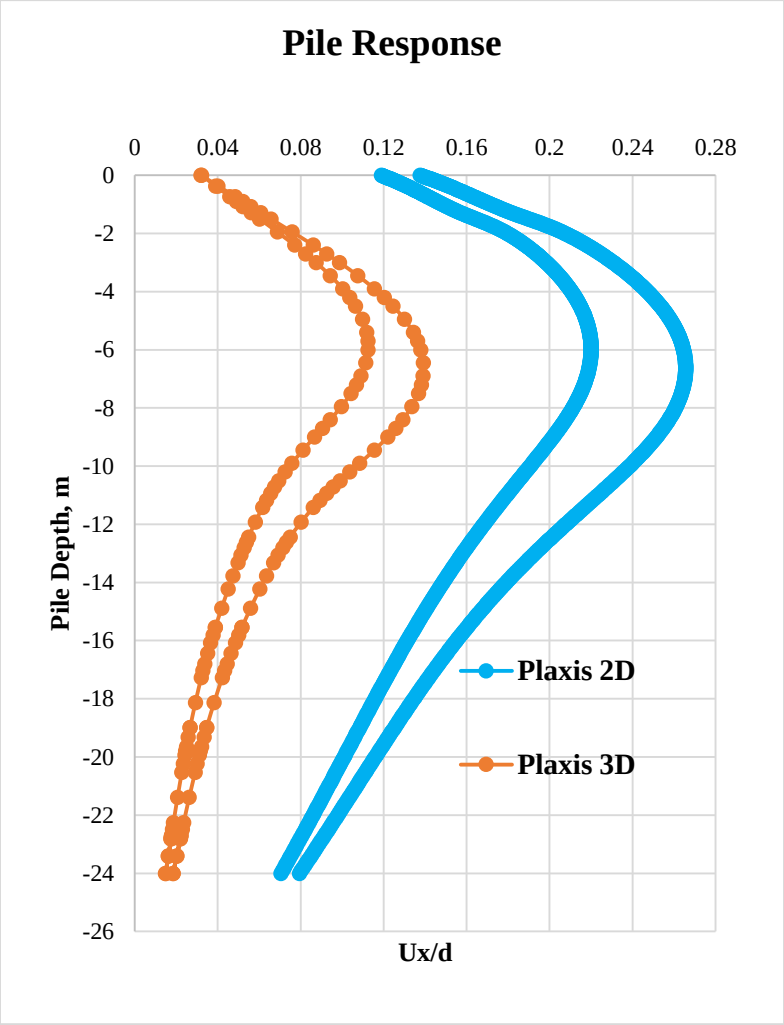

Figure 4-29 Comparison of displacement distribution of pile wall supporting Excavation by 2D and 3D FEM analysis

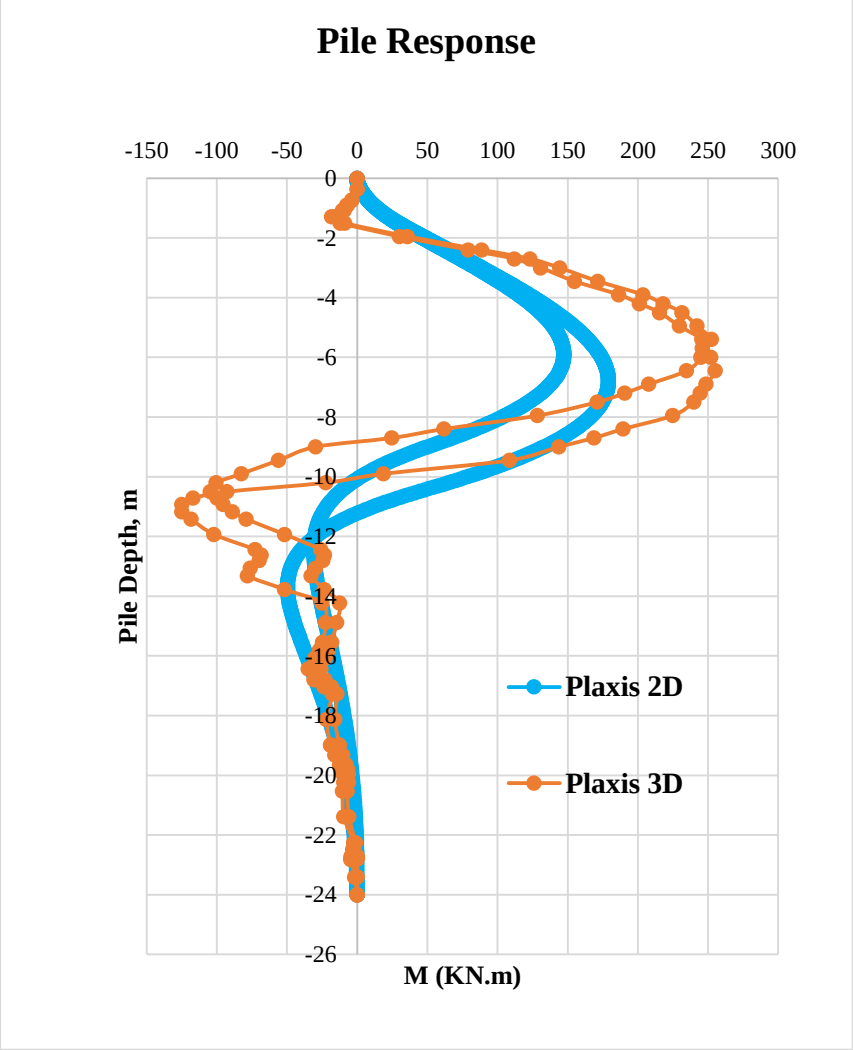

Figure 4-30 Bending moment distribution of pile wall supporting Excavation by 2D and 3D FEM analysis

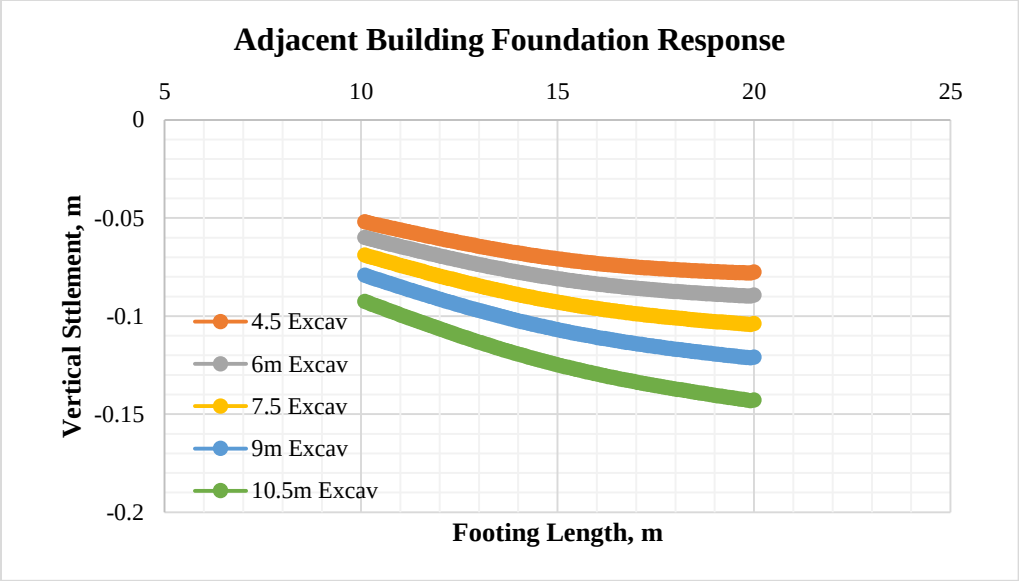

Figure 4-31 Vertical settlement of the building foundation for different excavation depths when supported with pile wall (Pile length 24m, Plaxis 2D)

From Figure 4-31 and Figure 4-32 it can be clearly seen that the vertical settlement of building foundation computed by 2D finite element analysis is greater than that of 3D FEM analysis result.

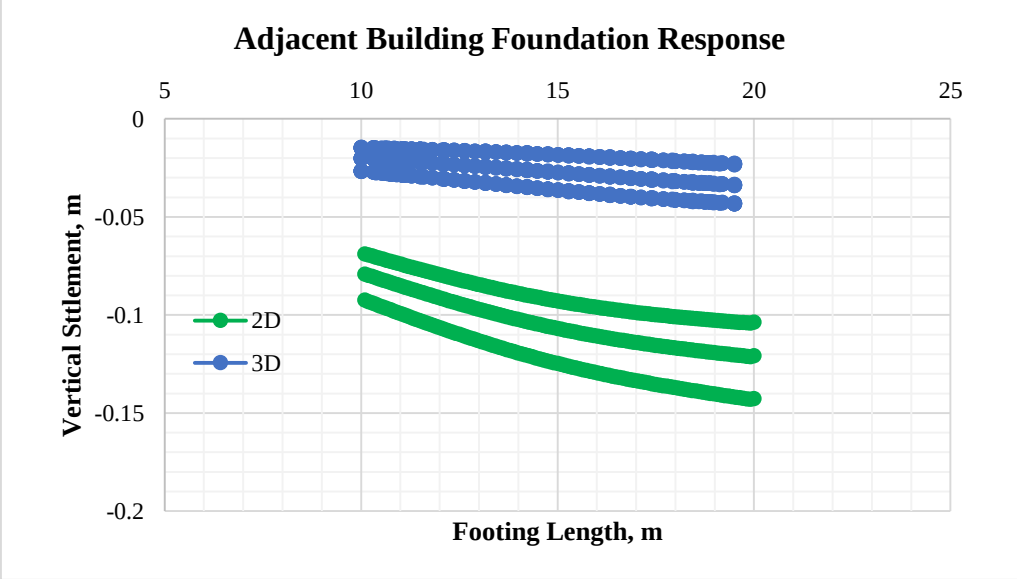

Figure 4-32 Comparison of Vertical settlement of the building foundation for different excavation depths when supported with pile wall (Pile length 24m, Plaxis 2D and Plaxis 3D)

5 CONCLUSION AND RECOMMENDATION

The outcomes of the parametric investigation are highlighted in this chapter along with potential justifications. The outcomes of the data analysis in this research are described, and thus the research purpose is met, as well as the inadequacies of this research, so that additional research can be carried out in the coming days, as research in the field of ground improvement in our nation is uncommon.

5.1 Conclusion

This study focused on investigating the performance of a cantilever pile wall as an excavation support system. Excessive excavation may be a major contributing element to the excessive motions that might occur when a cantilever stage is present during construction. To conduct the study, Finite Element Modeling (2D and 3D FEM) was employed. A parametric analysis was carried out, considering factors such as excavation depth, pile embedded depth, soil undrained shear strength, adjacent building foundation type, and stress on the foundation.

According to the study's findings, the stiffness of both the soil and the pile wall affects how the pile wall behaves. Among the three types of adjacent building foundations analyzed, isolated footing showed the highest lateral displacement of the pile wall and its vertical settlement. Therefore, when an isolated footing is present adjacent to the excavation, special attention should be given to its potential impact.

The usefulness of the cantilever pile wall in minimizing the vertical settling of the foundation of the neighboring structure was also investigated. The results demonstrated that the cantilever pile wall significantly reduces the vertical settlement and rotation of the footing. Additionally, according to observations, when the undrained shear strength rises, the lateral displacement and bending moment decrease, while they increase with higher adjacent building foundation stress.

A comparison between the analysis results obtained from 2D and 3D FEM was performed. The analysis conducted using Plaxis 2D showed higher deformation and bending values compared to those obtained from Plaxis 3D. Specifically, the maximum deflection computed by Plaxis 2D was found to be 92% greater than the maximum

deflection calculated by Plaxis 3D, and it was six times greater than the deflection of the corner pile in Plaxis 3D.

5.2 Recommendation

Due to time and resource constraints, various assumptions were made in order to carry out the parametric analysis. Some of the recommendations and future studies that can be carried out are addressed below:

The analysis was carried considering the average properties of soil, non-homogeneous soil model may be adopted for further study.

The soil modelling was done using the Mohr-Coulomb model although the other advance model can be used to replicate the real site condition.

Static loading has been used during the analysis. Dynamic loading may be applied to investigate the behavior of stone column.

References:

Arai, Y., Kusakabe, O., Murata, O., & Konishi, S. (2008). A numerical study on ground displacement and stress during and after the installation of deep circular diaphragm walls and soil excavation. *Computers and Geotechnics*, *35*(5), 791–807.

Bjerrum, L., & Eide, O. (1956). Stability of strutted excavations in clay. *Geotechnique*, *6*(1), 32–47.

Caquot, A. I., & Kérisel, J. L. (1948). *Tables for the calculation of passive pressure, active pressure and bearing capacity of foundations*. Gautier-Villars.

Clarke, B. G., & Wroth, C. P. (1984). Analysis of Dunton Green retaining wall based on results of pressuremeter tests. *Geotechnique*, *34*(4), 549–561.

Clough, G. W. (1990). Construction Induced Movements of Insitu Wall, Design and Performance of Earth Retaining Structure. *ASCE*, 439–479.

Clough, G. W., & Hansen, L. A. (1981). Clay anisotropy and braced wall behavior. *Journal of the Geotechnical Engineering Division*, *107*(7), 893–913.

Clough, G. W., Smith, E. M., & Sweeney, B. P. (1989). Movement control of excavation support systems by iterative design. *Foundation Engineering: Current Principles and Practices*, 869–884.

Dong, Y., Burd, H., Houlsby, G., & Xu, Z. (2013). 3D FEM modelling of a deep excavation case considering small-strain stiffness of soil and Thermal shrinkage of concrete. *Proceedings of the International Conference on Case Histories in Geotechnical Engineering*.

Fan, X., Phoon, K.-K., Xu, C., & Tang, C. (2021). Closed-form solution for excavation-induced ground settlement profile in clay. *Computers and Geotechnics*, *137*, 104266.

Fang, H.-Y. (2013). *Foundation engineering handbook*. Springer Science & Business Media.

Finno, R. J., Blackburn, J. T., & Roboski, J. F. (2007). Three-dimensional effects for supported excavations in clay. *Journal of Geotechnical and Geoenvironmental Engineering*, *133*(1), 30–36.

Finno, R. J., Harahap, I. S., & Sabatini, P. J. (1991). Analysis of braced excavations with coupled finite element formulations. *Computers and Geotechnics*, *12*(2), 91–114.

Fourie, A. B., & Potts, D. M. (1989). Comparison of finite element and limiting equilibrium analyses for an embedded cantilever retaining wall. *Geotechnique*, *39*(2), 175–188.

Godavarthi, V. R., Mallavalli, D., Peddi, R., Katragadda, N., & Mulpuru, P. (2011). Contiguous pile wall as a deep excavation supporting system. *Leonardo Electronic Journal of Practices and Technologies*, *19*, 144–160.

Goh, A. T. C., Zhang, F., Zhang, W., Zhang, Y., & Liu, H. (2017). A simple estimation model for 3D braced excavation wall deflection. *Computers and Geotechnics*, *83*, 106–113.

Hashash, Y. M. A., & Whittle, A. J. (1996). Ground movement prediction for deep excavations in soft clay. *Journal of Geotechnical Engineering*, *122*(6), 474–486.

Hashash, Y. M. A., & Whittle, A. J. (2002). Mechanisms of load transfer and arching for braced excavations in clay. *Journal of Geotechnical and Geoenvironmental Engineering*, *128*(3), 187–197.

Hou, Y. M., Wang, J. H., & Zhang, L. L. (2009). Finite-element modeling of a complex deep excavation in Shanghai. *Acta Geotechnica*, *4*, 7–16.

Hsieh, P.-G., & Ou, C.-Y. (1998). Shape of ground surface settlement profiles caused by excavation. *Canadian Geotechnical Journal*, *35*(6), 1004–1017.

Hsieh, P.-G., Ou, C.-Y., & Lin, Y.-L. (2013). Three-dimensional numerical analysis of deep excavations with cross walls. *Acta Geotechnica*, *8*, 33–48.

Hubbard, H. W., Potts, D. M., Miller, D., & Burland, J. B. (1984). Design of the

retaining walls for the M25 cut and cover tunnel at Bell Common. *Geotechnique*, *34*(4), 495–512.

Kung, G. T., Juang, C. H., Hsiao, E. C., & Hashash, Y. M. (2007). Simplified model for wall deflection and ground-surface settlement caused by braced excavation in clays. *Journal of Geotechnical and Geoenvironmental Engineering*, *133*(6), 731–747.

Lee, F.-H., Hong, S.-H., Gu, Q., & Zhao, P. (2011). Application of large three-dimensional finite-element analyses to practical problems. *International Journal of Geomechanics*, *11*(6), 529–539.

Lee, F.-H., Yong, K.-Y., Quan, K. C. N., & Chee, K.-T. (1998). Effect of corners in strutted excavations: Field monitoring and case histories. *Journal of Geotechnical and Geoenvironmental Engineering*, *124*(4), 339–349.

Long, M. (2001). Database for retaining wall and ground movements due to deep excavations. *Journal of Geotechnical and Geoenvironmental Engineering*, *127*(3), 203–224.

Long, M., Brangan, C., Menkiti, C. O., Looby, M., & Casey, P. (2012). Retaining walls in Dublin j. *Proceedings of the ICE: Geotechnical Engineering*, *165*, 247–266.

Mana, A. I., & Clough, G. W. (1981). Prediction of movements for braced cuts in clay. *Journal of the Geotechnical Engineering Division*, *107*(6), 759–777.

Ng, C. W. W., & Yan, R. W. M. (1999). Three-dimensional modelling of a diaphragm wall construction sequence. *Geotechnique*, *49*(6), 825–834.

O'rourke, T. D. (1993). Base stability and ground movement prediction for excavations in soft clay. In *Retaining structures* (pp. 657–686). Thomas Telford Publishing.

Orazalin, Z. Y., Whittle, A. J., & Olsen, M. B. (2015). Three-dimensional analyses of excavation support system for the Stata Center basement on the MIT campus. *Journal of Geotechnical and Geoenvironmental Engineering*, *141*(7), 5015001.

Ou, C.-Y. (2014). *Deep excavation: Theory and practice*. Crc Press.

Ou, C.-Y., Chiou, D.-C., & Wu, T.-S. (1996). Three-dimensional finite element analysis of deep excavations. *Journal of Geotechnical Engineering*, *122*(5), 337–345.

Ou, C.-Y., & Shiau, B.-Y. (1998). Analysis of the corner effect on excavation behaviors. *Canadian Geotechnical Journal*, *35*(3), 532–540.

Ou, C. Y., Lin, Y. L., & Hsieh, P. G. (2006). Case record of an excavation with cross walls and buttress walls. *Journal of GeoEngineering*, *1*(2), 79–87.

Peck, B. B. (1969). Deep excavation and tunnelling in soft ground, State of the art volume. *7th ICSMFE*, *4*, 225–290.

Pile foundation analysis and design. (1981). In *International Journal of Rock Mechanics and Mining Sciences & Geomechanics Abstracts* (Vol. 18, Issue 5, p. 100). https://doi.org/10.1016/0148-9062(81)90191-1

Poh, T. Y., & Wong, I. H. (1998). Effects of construction of diaphragm wall panels on adjacent ground: field trial. *Journal of Geotechnical and Geoenvironmental Engineering*, *124*(8), 749–756.

Poulos, H. G., & Chen, L. T. (1997). Pile Response Due to Excavation-Induced Lateral Soil Movement. *Journal of Geotechnical and Geoenvironmental Engineering*, *123*(2), 94–99. https://doi.org/10.1061/(asce)1090-0241(1997)123:2(94)

Poulos, H. G., Chen, L. T., & Hull, T. S. (1996). Model tests on single piles subjected to lateral soil movement. *Research Report - University of Sydney, School of Civil and Mining Engineering*, *723*, 1–28. https://doi.org/10.3208/sandf.35.4

Powrie, W., & Li, E. S. F. (1991). Finite element analyses of an in situ wall propped at formation level. *Geotechnique*, *41*(4), 499–514.

Ramadan, M. I., Ramadan, E. H., & Khashila, M. M. (2018). Cantilever Contiguous Pile Wall for Supporting Excavation in Clay. *Geotechnical and Geological Engineering*, *36*(3), 1545–1558. https://doi.org/10.1007/s10706-017-0407-5

Rankine, W. J. M. (1857). II. On the stability of loose earth. *Philosophical Transactions*

of the Royal Society of London, *147*, 9–27.

RHG, P. (1995). Mohr circles, stress paths and geotechnics. *E&FN Spon*.

Rishitha, A. L. (2015). *Numerical Modelling of Laterally Loaded Single Pile*. Indian Institute of Technology Hyderabad.

Samtani, N. C., & Nowatzki, E. A. (2006). *Soils and foundations: Reference manual*. United States. Federal Highway Administration.

Stewart, D. P., Jewell, R. J., & Randolph, M. F. (1994). Design of piled bridge abutments on soft clay for loading from lateral soil movements. *Geotechnique*, *44*(2), 277–296. https://doi.org/10.1680/geot.1994.44.2.277

Terzaghi, K. (1943). Theoretical Soil Mechanics John Wiley and Sons Inc. *New York*, *314*.

Terzaghi, K., Peck, R. B., & Mesri, G. (1996). *Soil mechanics in engineering practice*. John wiley & sons.

Wong, K. S., & Broms, B. B. (1989). Lateral wall deflections of braced excavations in clay. *Journal of Geotechnical Engineering*, *115*(6), 853–870.

Zdravkovic, L., Potts, D. M., & St John, H. D. (2005). Modelling of a 3D excavation in finite element analysis. *Geotechnique*, *55*(7), 497–513.

ANNEX